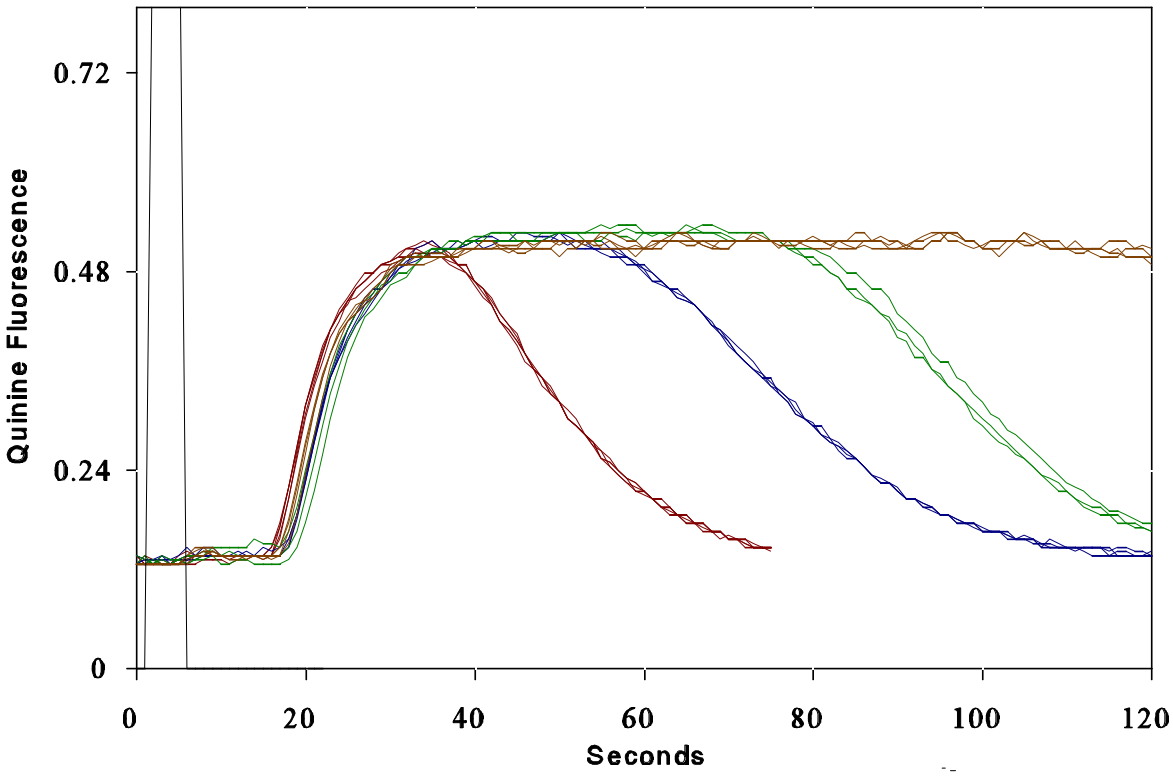

Figure 3.23. Small ByT-FAS raw data plots of a quinine tracer injected into the sample carrier stream.

Quinine sample was injected into the sample side of the system with different sample injection loop volumes in quadruplicate to determine when physical steady state is attained. The reagent and sample carrier stream ratio of flow rates of 10/1 (25/2.5 mL syringes). Total system flow rate of 0.22 mL/min. Sample side of ByT-FAS critical flow area tubing internal diameters of 0.0025" (64 microns) i.d. — 5 *u*L sample loop, — 10 *u*l sample loop, — 15 *u*L sample loop, — 25 *u*L sample loop.

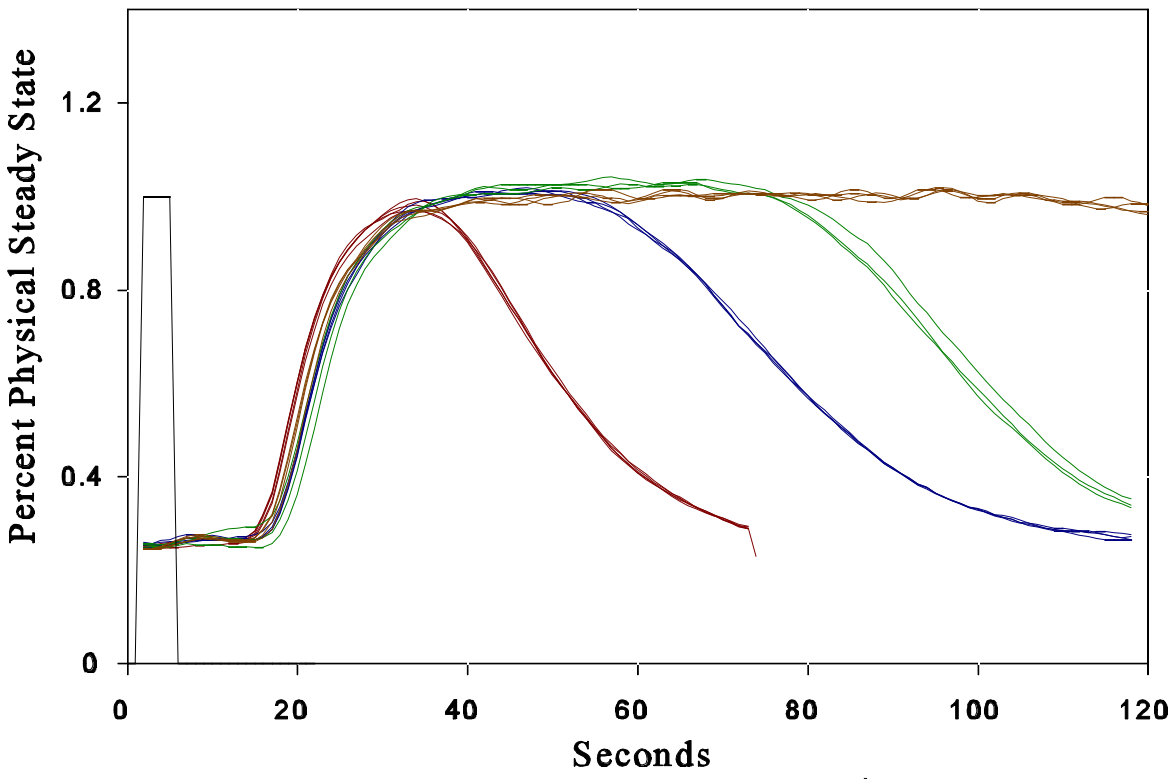

Figure 3.24. Small ByT-FAS raw data traces expressed as a percent of physical steady state.

Running box car average (OOXOO) expressed as a percentage of the physical steady state signal of a quinine tracer injected into the sample carrier stream in quadruplicate. Reagent and sample carrier stream ratio of flow rates of 10/1 (25/2.5 mL syringes). Total system flow rate of 0.22 mL/min. Sample side of ByT-FAS critical flow area tubing internal diameters of 0.0025" (64 microns) i.d. — 5 *u*L sample loop, — 10 *u*l sample loop, — 15 *u*L sample loop, — 25 *u*L sample loop.

loop. This increase in length can alter the back pressure of the system. This could explain why the time of physical steady state attainment is different. The 10 and 15 *u*L sample loops show no time difference whatsoever.

The precision of achievement of physical steady state between runs was also good. The times that physical steady state were attained for a certain volume varied only by one to two seconds from run to run. However, if a trapping mechanism at physical steady state concentrations is to be used, the trapping valve should be programmed to fire at least five seconds after the approximate attainment of physical steady state to allow for sample to sample variance in reaching the absolute measurement.

The use of 0.0025" internal diameter tubing on the sample side of the system caused frequent problems with particulate matter blockage of the system. Also, the system back pressure was large and frequently caused system component failures. As a result, the sample side tubing was replaced with 0.005" internal diameter tubing to alleviate these problems.

2.7 Low Molecular Weight Analyte; Effects of Sample Volume on Reaching Physical Steady State With 0.005" Sample Side Tubing Internal Diameter

Shown in Figure 3.25 are quinine traces in triplicate expressed as a percentage of physical steady state from injected volumes of 10, 15, and 25 *u*L into the sample carrier flow stream. The reagent to sample carrier stream flow ratio was 10/1. The percent of physical steady state data were calculated from the average signal of the 25 *u*L injections between 50 and 110 seconds of the run. This experiment was identical to experiment 2.6 (Table 3.5) except that the sample side tubing internal diameter is 0.005", not 0.0025" i.d. The time interval that each injected volume was calculated to be at physical steady state is shown in Table 3.6.

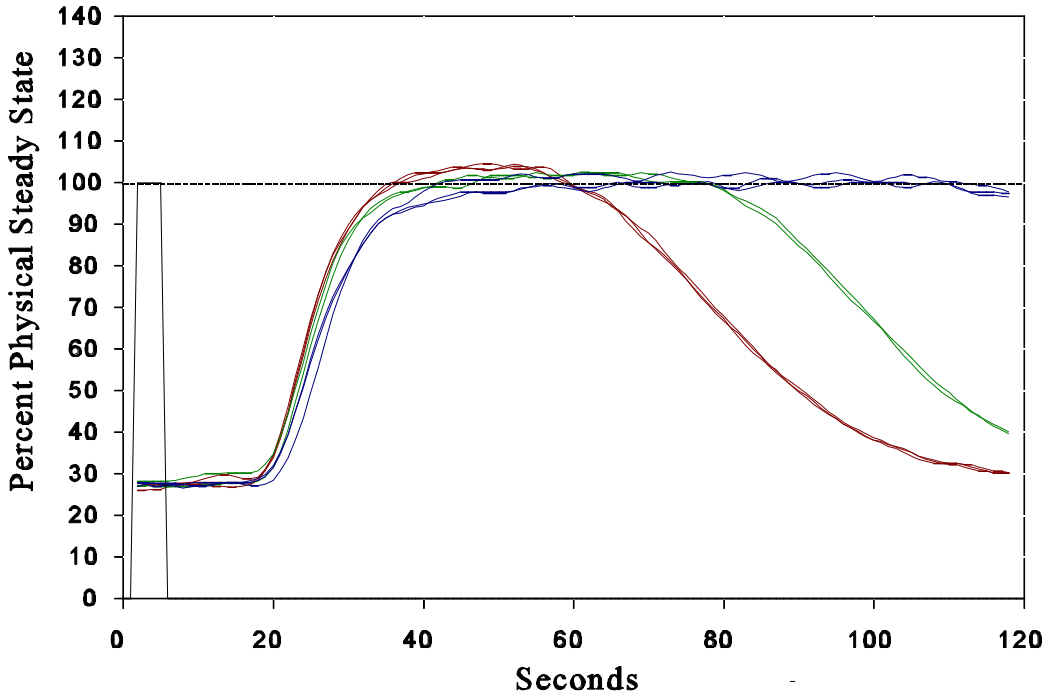

Figure 3.25. Small ByT-FAS system injection of a low molecular weight analyte into the sample carrier flow stream for attainment of physical steady state.

Quinine injection into the sample carrier flow stream with sample coil volumes of 10, 15 and 25 *u*L. Total system flow rate 0.22 mL/min. Reagent to sample carrier stream flow ratio of 10/1 (25/2.5 mL syringes). Sample side of ByT-FAS system tubing i.d.s of 0.005" not 0.0025". — 10 *u*L sample loop, — 15 *u*L sample loop, — 25 *u*L sample loop,

Table 3.6 Seconds of run that sample reaches physical steady state for a 10/1 flow ratio and 0.005" sample side tubing internal diameter.

	Injected Volumes		
Run	10 *u*L	15 *u*L	25 *u*L
1	37 - 59 s	41 - 79 s	55 - 111 s
2	37 - 59 s	41 - 79 s	55 - 110 s
3	36 - 59 s	XX	42 - 115 s

From the data in Table 3.6 it is apparent that increasing the sample side tubing internal diameter from 0.0025" to 0.005" makes a noticeable difference in the attainment and duration of physical steady state. The 10 *u*L injection time intervals were virtually identical to those in Table 3.5. However, the 15 *u*L injections took about four seconds longer to reach physical steady state than those in Table 3.5. The largest difference was apparent in the 25 *u*L injections. These differences are partially attributable to the greater sample dispersion that occurs in the larger internal diameter tubing. Also, while the sample side flow rate was the same as in experiment 2.6, the rate of transport to the detector was slower because of the larger volume in the sample side tubing. The differences in the data reflected a combination of factors, back pressure, laminar dispersion, and sample coil variance that can impact the attainment of physical steady state.

2.8 Low Molecular Weight Analyte; Effects of Sample Volume on Reaching Physical Steady State With a Reagent to Sample Carrier Flow Stream Ratio of 5/1.

Shown in Figure 3.26 are quinine traces in quadruplicate expressed as a percentage of physical steady state from injected volumes of 10, 15, and 25 *u*L into the sample carrier flow stream. The reagent to sample carrier stream flow ratio was 5/1. The percent of physical

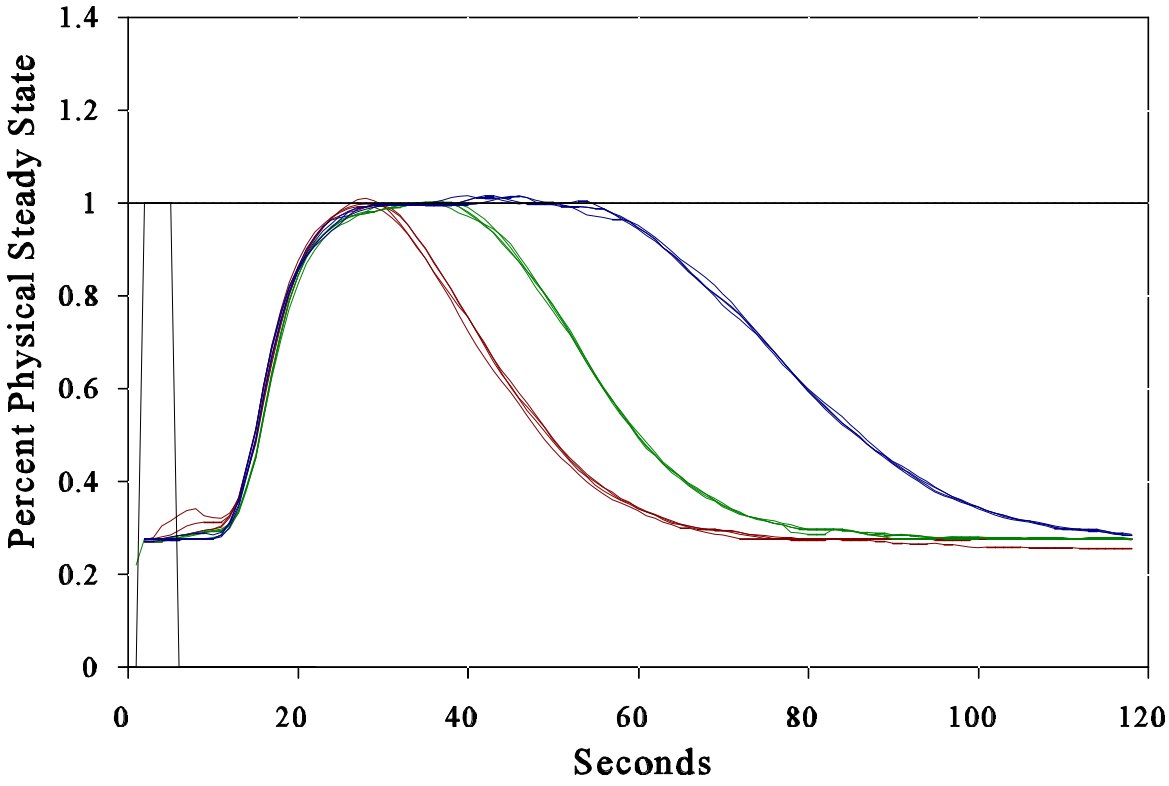

Figure 3.26. Small ByT-FAS system injection of a low molecular weight analyte into the sample carrier flow stream for the time to reach physical steady state.

Quinine injection into the sample carrier flow stream with sample coil volumes of 10, 15 and 25 *u*L. Total system flow rate 0.24 mL/min. Reagent to sample carrier stream flow ratio of 5/1 (25/5 mL syringes). Sample side tubing i.d. is 0.005". — 10 *u*L sample loop, — 15 *u*L sample loop, — 25 *u*L sample loop.

steady state data were calculated from the average signal of the 25 *u*L injections between 30 and 50 seconds of the run. From this data, the time interval that each injected volume attains a physical steady state signal can be tabulated. Shown in Table 3.7 are the time intervals that

Table 3.7 Seconds of run that sample reaches physical steady state for a 5/1 flow ratio and 0.005" sample side tubing internal diameter.

	Injected Volumes		
Run	10 *u*L	15 *u*L	25 *u*L
1	28 - 31 s	30 - 39 s	28 - 56 s
2	26 - 30 s	29 - 38 s	27 - 56 s
3	26 - 30 s	30 - 40 s	27 - 52 s
4	26 - 29 s	30 - 39 s	27 - 56 s

each injection shown in Figure 3.26 was calculated to be at physical steady state.

The higher sample carrier stream flow rate facilitated the achievement of a physical steady state signal more quickly than experiments 2.6 and 2.7. However, the injected sample boluses did not stay at physical steady state as long. As total system flow rates increase, the sample and reagent volumes necessary will also increase.

Assay systems that require a high sample throughput will operate on ByT-FAS with a high total flow rate. However, the achievement and duration of physical steady state is affected at this high flow rate.

Conversely, assay systems that require small sample and reagent volumes will need to be performed with a slower total flow rate (experiments 2.6 and 2.7). As a result, sample throughput will be diminished. If the priority of a certain ByT-FAS application is high sample throughput, then the faster flow rate will enable a shorter analysis time per sample. However, there is a corresponding compromise in the injected volume size necessary to achieve a physical steady state signal. Depending on the priority, sample throughput or volume, is the most important for a given assay, ByT-FAS can be designed to accommodate it.

2.9 Low Molecular Weight Analyte; Effects of Sample Volume on Reaching Physical Steady State With Reagent to Sample Flow Stream Ratio of 2.5/1

Shown in Figure 3.27 are quinine traces in quadruplicate expressed as a percentage of physical steady state from injected volumes of 15, 25, and 50 *u*L into the sample carrier flow stream. The reagent to sample carrier stream flow ratio was 2.5/1. The percent of physical steady state data were calculated from the average signal of the 50 *u*L injections between 20 and 50 seconds of the run. From this data, the time interval that each injected volume attained a physical steady state signal can be tabulated. Shown in Table 3.8 are the time intervals that each injection shown in Figure 3.27 was calculated to be at physical steady state.

The 15 *u*L sample injections achieved physical steady state in 3 out of 4 of the runs for about 3

seconds. Because the four 15 *u*L runs did not all reach physical steady state, it would be imprudent to attempt routine assays for absolute measurement with a 15 *u*L injection at this flow rate (reagent to sample carrier stream flow ratio of 2.5/1).

However, if injected sample volume is not a priority consideration, then a 25 or 50 *u*L

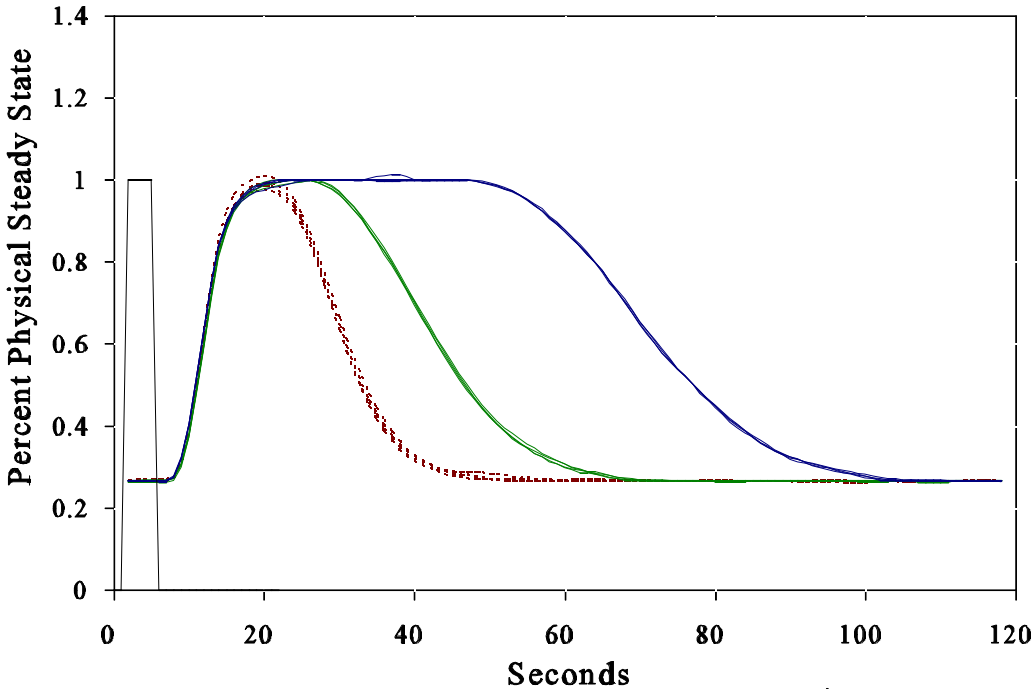

Figure 3.27. Small ByT-FAS system injection of a low molecular weight analyte into the sample carrier flow stream for the time to reach physical steady state.

Quinine injection into the sample carrier flow stream with sample coil volumes of 15, 25 and 50 *u*L. Total system flow rate 0.28 mL/min. Reagent to sample carrier stream flow ratio of 2.5/1 (25/10 mL syringes). Sample side tubing i.d. of 0.005". —15 *u*L sample loop, — 25 *u*L sample loop, — 50 *u*L sample loop,

Table 3.8 Seconds of run that sample reaches physical steady state for a 2.5/1 flow ratio and 0.005" sample side tubing internal diameter.

	Injected Volumes		
Run	15 *u*L	25 *u*L	50 *u*L
1	17 - 22 s	20 - 28 s	20 - 51 s
2	19 - 22 s	22 - 28 s	20 - 50 s
3	19 - 21 s	20 - 28 s	23 - 51 s
4	0 s	19 - 28 s	19 - 51 s

sample injection can attain physical steady state in about 20 seconds. This is much earlier than the flow ratios of 10/1 (experiment 2.7) and 5/1 (experiment 2.8), which required 55 and 30 seconds, respectively, to reach a physical steady state signal.

2.10 High Molecular Weight Analyte; Effects of Reagent Volume on Reaching Physical Steady State With Reagent to Sample Flow Stream Ratio of 10/1

Shown in Figure 3.28 are FITC-BSA traces in triplicate expressed as a percentage of physical steady state from injected volumes of 100 and 125 *u*L into the reagent carrier flow stream. The reagent to sample carrier stream flow ratio was 10/1. The percent of physical steady state data were calculated from the average signal of the 125 *u*L injections between 30 and 50 seconds of the run.

The 125 *u*L injection shows a physical steady state attainment of 30 to 50 seconds. From experiment 2.7 (Table 3.6), a 15 *u*L injection of a low molecular weight analyte at a 10/1 reagent to sample carrier stream flow ratio has a physical steady state signal from 41 to 79 seconds. As a result, when 125 *u*L of high molecular weight reagents and 15 *u*L of low molecular weight samples were injected into a 10/1 reagent to sample flow ratio, their absolute

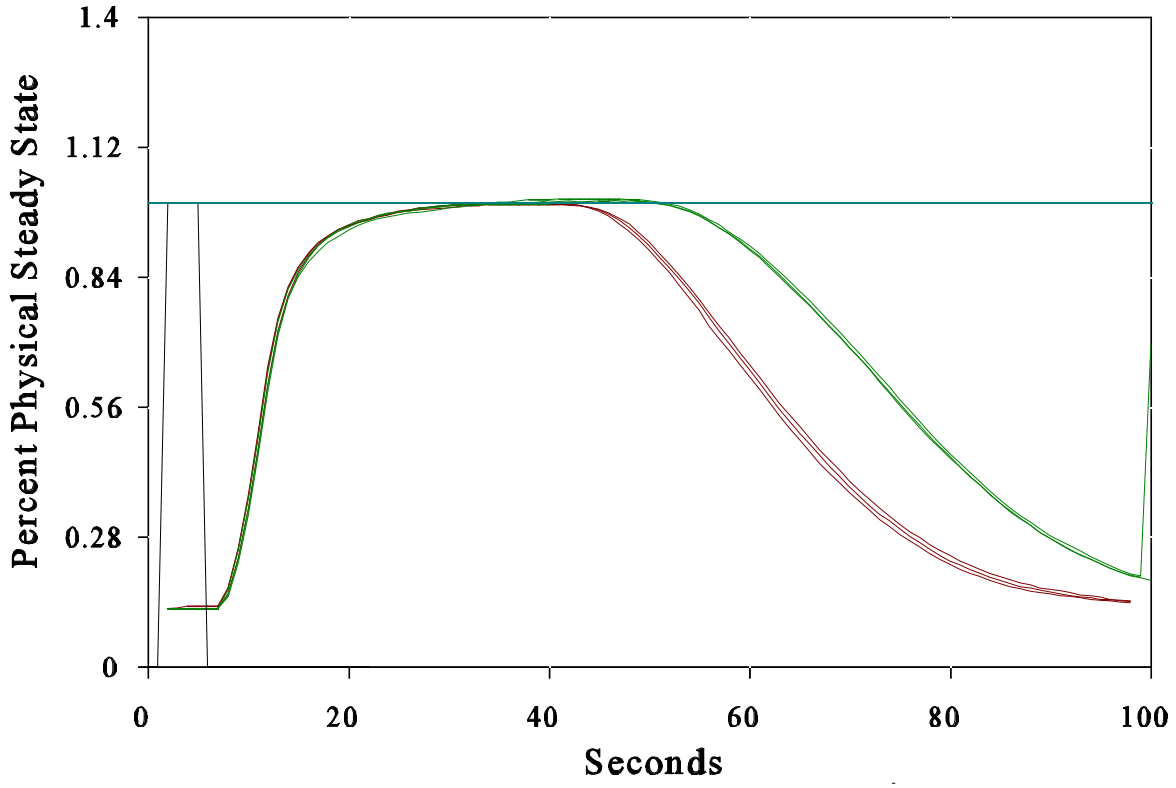

Figure 3.28. Small ByT-FAS system injection of high molecular weight tracer (FITC-BSA) into the reagent carrier stream.

Assay of two different reagent coil volumes, 100 and 125 *u*L to reach physical steady state with a high molecular weight analyte injected into the reagent side of the system. Reagent to sample carrier stream flow ratio of 10/1. Total system flow rate 0.22mL/min. — 100 *u*L reagent loop, — 125 *u*L reagent loop.

signals overlapped between 41 and 50 seconds. Consequently, a trapped mixture of reagent and sample at 45 seconds into the ByT-FAS run resulted in simultaneous physical steady state signal for both the reagent and sample boluses.

2.11 Calibration of the Age of an Enzyme Reaction at the Time of Trapping at Physical Steady State

Shown in Figure 3.29 is a raw data plot of a sample control, enzyme control, and an enzyme kinetic trace of G6PDH with $NADP^+$ and glucose-6-phosphate. From the enzyme and substrate injection at physical steady state, the fluorescence signal corresponds to the amount of product that has been produced so far in the reaction. At the point of trapping at 40 seconds into the run, the kinetic rate is monitored, which corresponds to the rate of product production. From the data in Figure 3.29, using a linear back extrapolation to zero fluorescence, which should be zero time for the enzyme reaction assuming no lag phase, the age of the enzyme reaction at the point of trapping is approximately 3 seconds. This is drastically different than the age of the ByT-FAS run of 40 seconds at the point of trapping.

Knowing the age of enzyme catalyzed reaction is important in determining whether or not the measured velocity is an initial velocity as required by Michaelis-Menten kinetics for the evaluation of enzyme kinetic parameters.

2.12 Coupled Enzyme Kinetic Fast Glucose Assay Standard Curve Development

Shown in Figure 3.30 are the raw data kinetic traces used to generate the standard curve shown in Figure 3.31. Notice the characteristic coupled enzyme lag phase of each kinetic trace from 45 to 60 seconds of each run. As a consequence of this lag phase, the regression analysis of each data set was taken between 60 and 80 seconds to determine the enzyme velocity. The raw data also show good precision for duplicate runs of the same glucose concentration.

Shown in Figure 3.31 is a standard curve of hexokinase velocity versus glucose

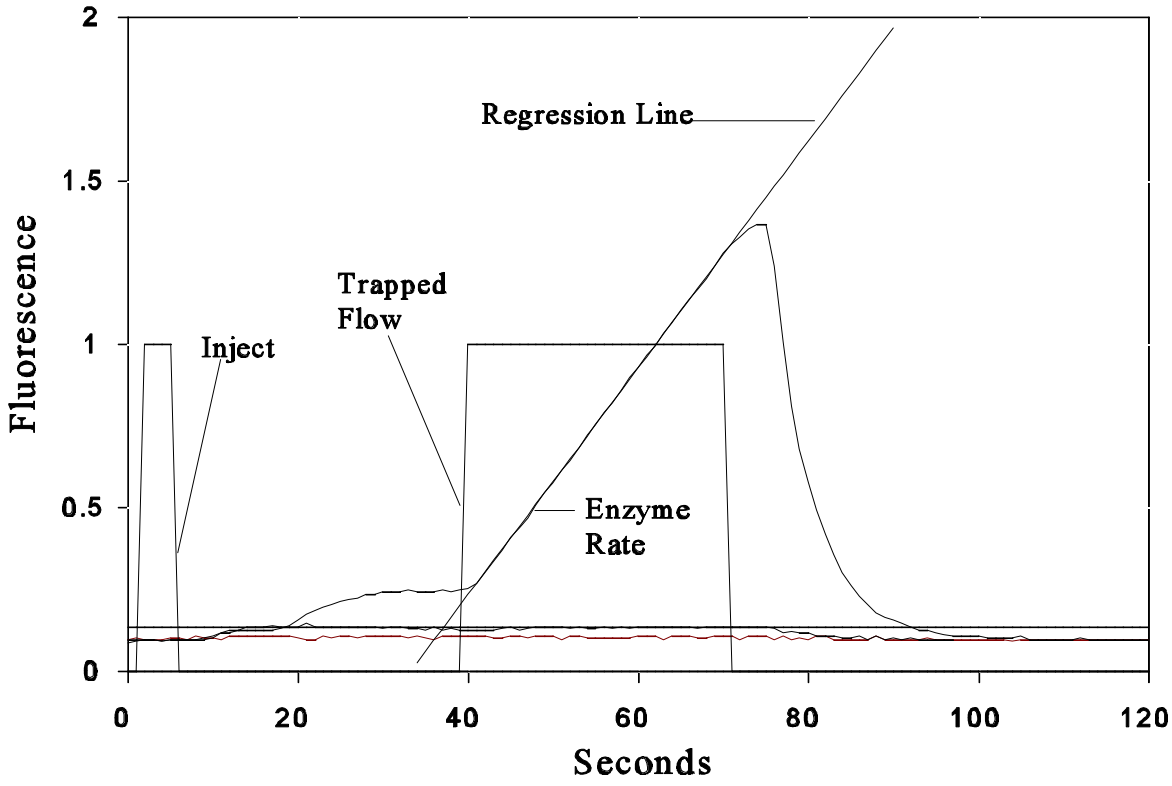

Figure 3.29. Small ByT-FAS system calibration of the age of an enzyme reaction at the time of trapping at physical steady state.

One enzyme catalyzed reaction. The product signal at physical steady state is equivalent to the amount of product produced so far and the reaction rate in the trapped time is the rate of production. Age of enzyme reaction is about 3 seconds old. Reagent and sample carrier stream flow ratio of 10/1. Total system flow rate of 0.22 mL/min.

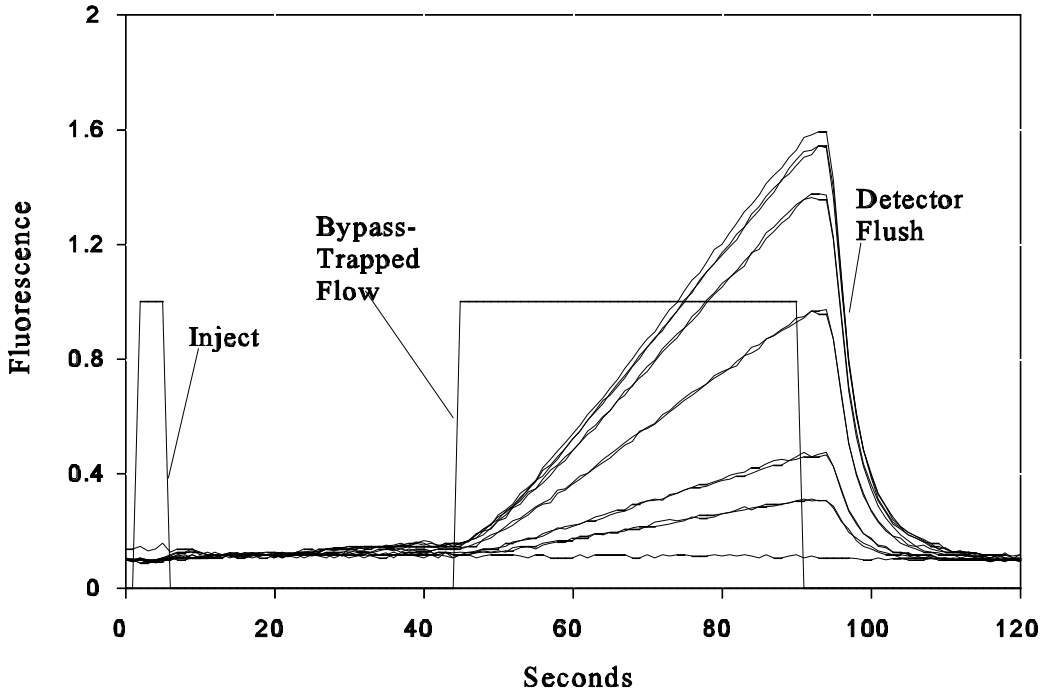

Figure 3.30. Small ByT-FAS system fast kinetic coupled enzyme glucose assay raw data traces of hexokinase velocity.

Glucose concentrations of 0, 5, 10, 25, 40, and 50 *u*M were measured at the point of detection from sample injection into the sample carrier flow stream in duplicate. Enzymes and additional non-rate limiting amounts of substrates were injected into the reagent carrier stream. 15 *u*L of sample and 125 *u*L of reagent injected into their respective carrier streams for each assay run. Reagent to sample carrier stream flow ratio of 10/1 (25/2.5 mL syringes). Total system flow rate of 0.22 mL/min.

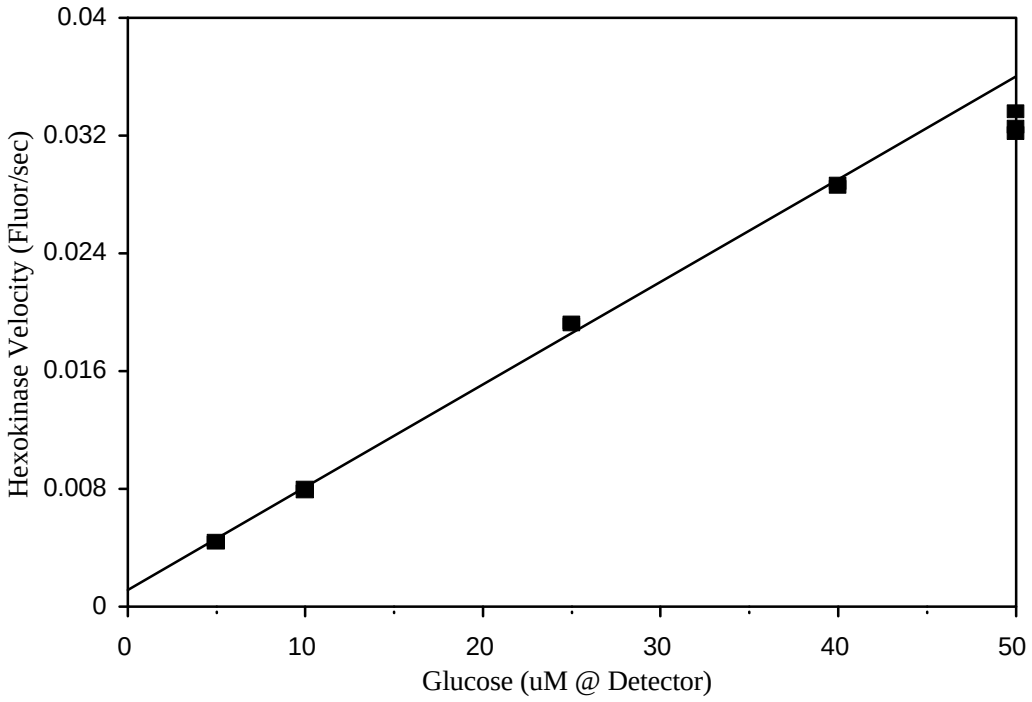

Figure 3.31. Small ByT-FAS system determined linear range of standard curve for the coupled enzyme kinetic glucose assay.

Small ByT-FAS system generated enzyme kinetic glucose standard curve of glucose concentrations at the point of detection. Plot of hexokinase velocity versus glucose concentration at the point of detection represents the approximate first order region of the Michaelis-Menten plot. Linear range of the enzyme kinetic glucose standard curve is 2.13 - 40 *u*M. — Regression line.

concentration. The Km of glucose with hexokinase as determined above is 154 *u*M at pH 7.4. From Michaelis-Menten kinetics, the first-order enzyme reaction rate is at substrate concentrations several fold less than the Km value of the substrate. As a guideline, substrate concentrations of 1/3 or less the Km value should approximate a first-order response with respect to enzyme velocity. For a Km value of 154 *u*M, a linear response of enzyme velocity to substrate concentration should be observed from 0 to 50 *u*M glucose.

From Figure 3.31, the glucose concentrations that produce a linear hexokinase response were 2.13 - 40 *u*M. The 50 *u*M glucose concentration began to deviate away from an approximate first-order kinetic response.

2.13 Comparison of Method of Standard Additions for Manual Colorimetric and ByT-FAS Kinetic Assay of Starch in a Mixed Diet Food Composite

Shown in Figure 3.32 is a standard response curve and a standard additions curve for determination of any mixed diet food composite interference on the reaction chemistry of the manual colorimetric end-point method. Because the standard additions data regression slope is parallel to the standard response regression slope, it can be concluded that there is no matrix interference on the manual end-point reaction chemistry.

However, shown in Figure 3.33 is a standard response curve and a standard additions curve to determine any effects of a mixed diet composite on a ByT-FAS fast enzyme kinetic assay of glucose. The two sets of data do not have parallel regression lines, which indicates interference from the mixed diet composite on the enzyme kinetic assay.

Even though the same samples were used to generate the data shown in Figures 3.32 and 3.33, the manual end-point assay showed no matrix interference, while the ByT-FAS enzyme kinetic method clearly showed interference.

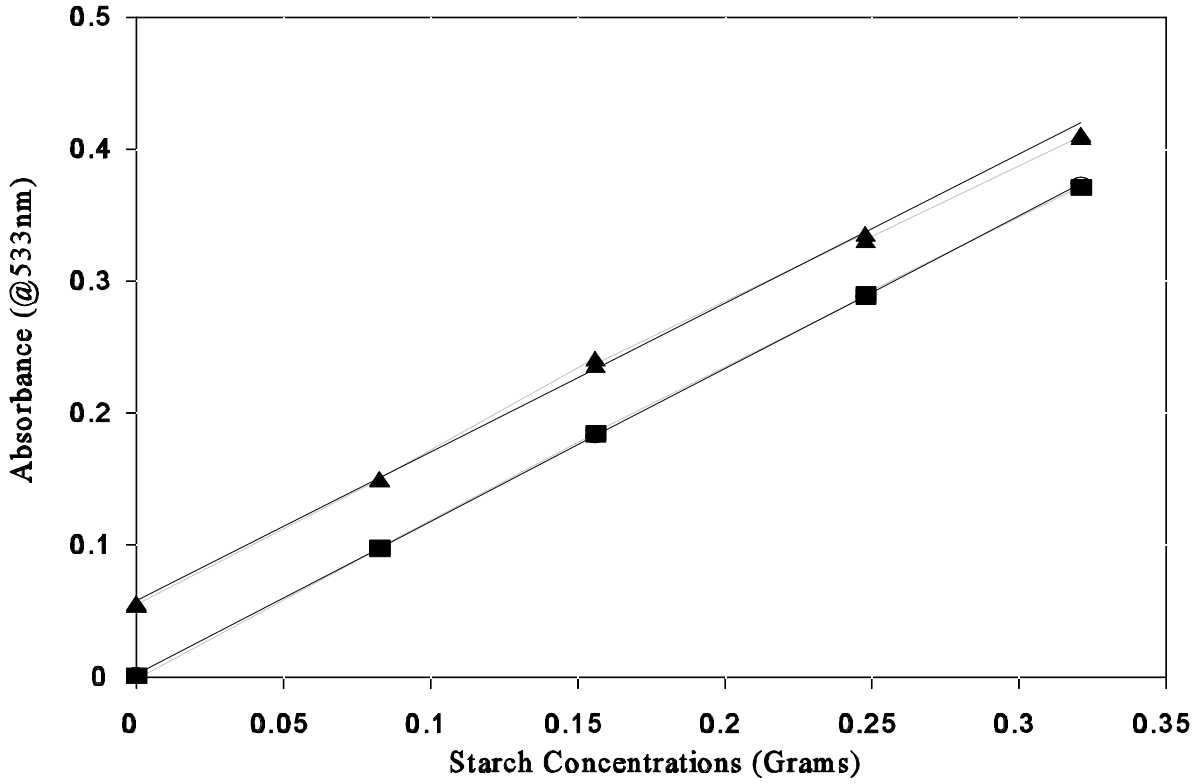

Figure 3.32. Manual colorimetric equilibrium enzyme assay spiking experiment to determine any interference of food composite matrix on the glucose assay chemistry.

The manual colorimetric end-point assay was investigated with a mixed-diet food matrix for any matrix interferences on the quantitation of glucose. This assay was not performed using ByT-FAS. The food matrix did not exhibit interference on the assay chemistry because the parallel regression lines indicate that the added starch in the food matrix was fully recovered. ■ - Standard response (standard curve) data, ▲ - Standard additions (spiked) data.
— Regression lines.

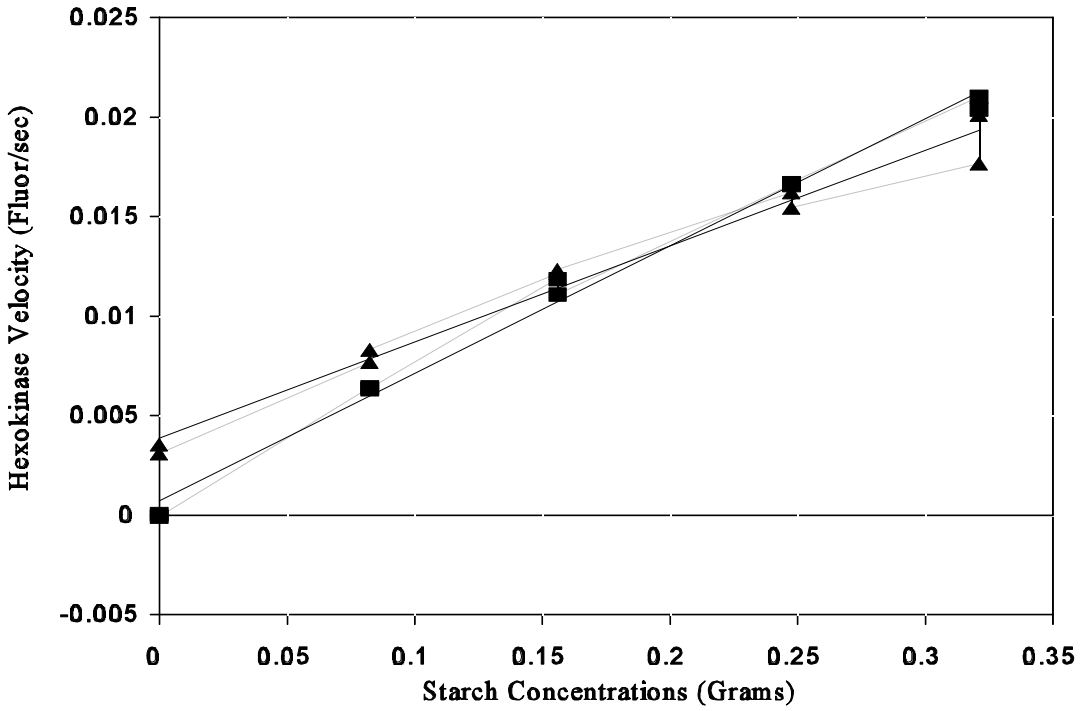

Figure 3.33. Small ByT-FAS coupled enzyme kinetic glucose assay spiking experiment to determine any interference of food composite matrix on assay chemistry.

The hexokinase enzyme kinetic glucose assay with ByT-FAS was investigated with a mixed-diet food matrix for any matrix interferences on the quantitation of glucose. The food matrix interfered with the quantitation of glucose because the non-parallel regression lines indicate that the added starch in the food matrix was not fully quantitated by the kinetic enzyme assay. ■ - Standard response (standard curve) data, ▲ - Standard additions (spiked) data.
— Regression lines.

2.14 Method of Standard Additions for the ByT-FAS Coupled Enzyme Kinetic Assay of Glucose in Heparinized Canine Plasma

Shown in Figure 3.34 is the ByT-FAS standard response curve and a standard additions curve to elucidate any interference of a canine heparinized plasma matrix on the reaction chemistry of the fast hexokinase enzyme method for quantification of glucose. Because the standard additions data regression slope was parallel to the standard response regression slope, it can be concluded that there was no matrix interference on the assay chemistry.

Using the enzyme kinetic method, the plasma glucose concentration of several canine samples were assayed for comparison to the values of the same samples determined at the Virginia-Maryland College of Veterinary Medicine. Sample glucose values are reported with the 2σ of the total assay for a direct comparison of the Veterinary School data with the ByT-FAS enzyme kinetic method. The values as determined by the veterinary school and the ByT-FAS enzyme kinetic method are shown in Table 3.9.

Table 3.9 Comparison of ByT-FAS versus Veterinary School determinations for glucose in canine heparinized plasma.

	Sample 1	Sample 2
	Plasma glucose (mg/dL ± 2 S.D.)	Plasma glucose (mg/dL ± 2 S.D.)
Veterinary School	102 ± 7.14	93 ± 6.51
ByT-FAS	117 ± 6.57	103.6 ± 6.11

Although the different methods yield different means, the data compared with their corresponding 2σ values are not that dissimilar. When the method and laboratory variances are taken into account, the data appear comparable between the two methods.

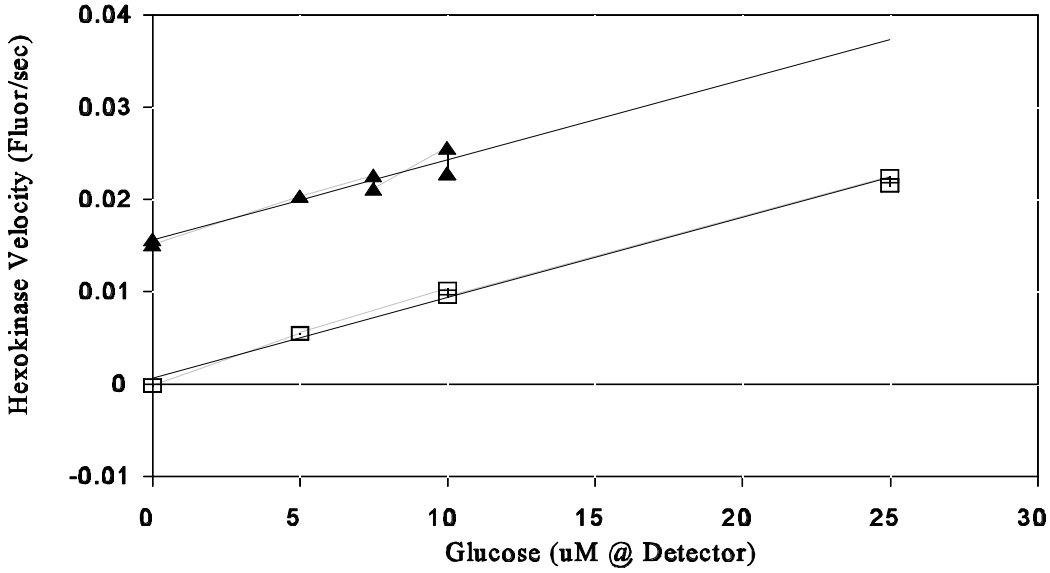

Figure 3.34. Small ByT-FAS coupled enzyme kinetic glucose assay spiking experiment to determine interference of canine plasma matrix on the assay chemistry.

The hexokinase enzyme kinetic glucose assay with ByT-FAS was investigated with a canine heparinized plasma matrix for any matrix interferences on the quantitation of glucose. The plasma matrix did not interfere with the quantitation of glucose because the parallel regression lines indicate that the added glucose in the plasma matrix was fully quantitated by the kinetic enzyme assay. Parallel lines indicate that there is no assay matrix interference on the assay chemistry. □ - Standard response (standard curve) data, ▲ - Standard additions (spiking) data. — Regression lines.

2.15 Fast Equilibrium Coupled Enzyme Assay of Cholesterol; Standard Curve Development

In Figure 3.35 are the raw data traces that were used to generate the standard curve for Figure 3.36. Shown in Figure 3.36 is the standard curve of cholesterol generated from the fast equilibrium enzyme assay. Notice the fast attainment of reaction equilibrium after the point of trapping at about 60 seconds into the run.

While the standard curve in Figure 3.36 has good precision and linearity, there are several characteristics of the raw data traces in Figure 3.35 that indicate problems with the cholesterol assay run on ByT-FAS. First, the non-blank samples appear to crossover to the next sample as indicated by the signal hump at 15 seconds into the run. Also, while the enzyme equilibrium data have good precision, the attainment of physical steady state stage does not show good precision for duplicate samples. Lastly, at the system flush stage approximately 90 seconds into the run, there was a large post-trap spike in fluorescence signal for the samples that only occurred with this assay. The post-trap spike in signal had not been observed in any other assay type performed on ByT-FAS. It could possibly be a higher concentration portion of the bolus which would indicate that the trapping time is not set to measure a physical steady concentration. However, regardless of any change in the trapping time, the signal still occurs.

For this assay, the sample carrier flow stream and injected sample solutions are non-aqueous (95% ethanol), while the reagent carrier flow stream is an aqueous buffer. When the sample solutions containing cholesterol were mixed in the aqueous buffer in a test tube at the same ratio occurring in ByT-FAS (10/1), some precipitate was observed in the solution. This suggests that the cholesterol may be precipitating in ByT-FAS and/or sticking to various parts of the ByT-FAS system.

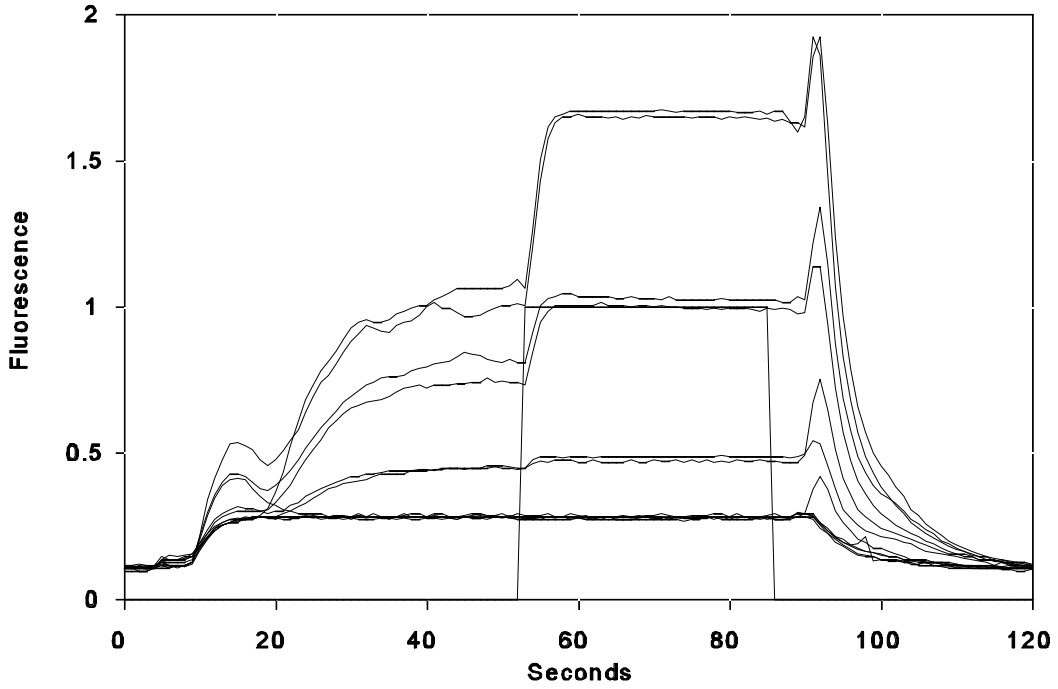

Figure 3.35. Small ByT-FAS system raw data for fast enzyme equilibrium cholesterol assay.

The small ByT-FAS system fast enzyme equilibrium cholesterol assay was run for concentrations of 0, 1.1, 4.1, and 8.2 *u*M cholesterol at the point of detection in duplicate. Increasing detector signal during the trapped phase of the run indicates higher cholesterol concentration. The spikes in signal at approximately 15 and 95 seconds indicate sample crossover between ByT-FAS runs.

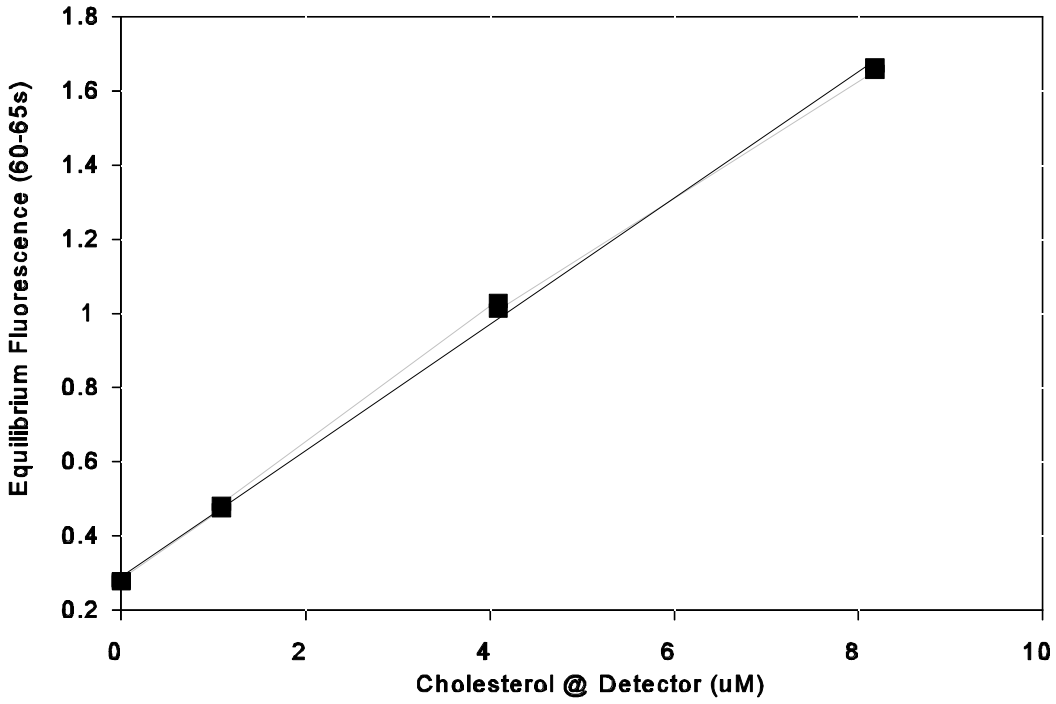

Figure 3.36. Small ByT-FAS system standard curve of cholesterol for fast equilibrium enzyme assay.

Small ByT-FAS system generated standard curve of enzyme equilibrium fluorescence versus cholesterol concentration at the point of detection. Cholesterol standards were dissolved in 95% ethanol. Sample carrier flow stream solution was 95% ethanol. Reagent carrier flow stream was aqueous buffer. The cholesterol standard curve had an $R^2 = 0.99853$, and LOD = 0.38 *u*M cholesterol.

2.16 Chemiluminescent Assay of ATP with Firefly Luciferase

Shown in Figure 3.37 are raw data traces of luciferase light signal as a function of time into the ByT-FAS run. Notice that during the trapped phase the light signal stays constant. This signal corresponds to a constant production of light as the reaction progresses. However, the individual photons are transient.

Light is a transient product of the luciferase catalyzed reaction with ATP, luciferin, and O_2. Consequently, the Y-axis data for Figure 3.38 was determined by summing the light signal from the detector during the trapped phase as if the product were accumulating in the detector cell as the reaction progressed. The rate of luciferase light production can be calculated from the summed light data by regression analysis during the trapped phase of the ByT-FAS run. These rates of light production from the slope of the regression analysis can then be plotted versus ATP concentration to yield a standard curve.

Shown in Figure 3.38 is the standard curve of ATP generated from the luciferase assay run on ByT-FAS. The standard curve has a linear range of 9.7 - 275 nM for ATP with the concentration at the point of detection. The R^2 for the linear range of the standard curve is 0.999.

2.17 Whole *E. coli* cell Chemiluminescent Assay of Genetic Transcription Levels

Shown in Figure 3.39 are the raw data traces of luciferase light production with different tetracycline induction concentrations in the overnight growth media. The colored pairs (duplicates) of lines correspond to the amount of tetracycline in the overnight culture. Increasing light signal corresponds to higher concentrations of tetracycline and more luciferase transcribed per cell. The raw data traces contain substantial detector noise as a result of the increased sensitivity needed to detect light production from inside the cells.

.Because light is a transient product of the luciferase catalyzed reaction with ATP, luciferin, and O_2, there is not an accumulation of detectable product. Alternatively, light intensity signal can be summed as if the light were accumulating. This gives the total amount of light produced per culture during the trapped phase of the ByT-FAS run. The summed light intensities of the raw data traces during the trapped phase of the run are shown in Figure 3.40. When the light intensities were summed, the high detector noise visible from the raw

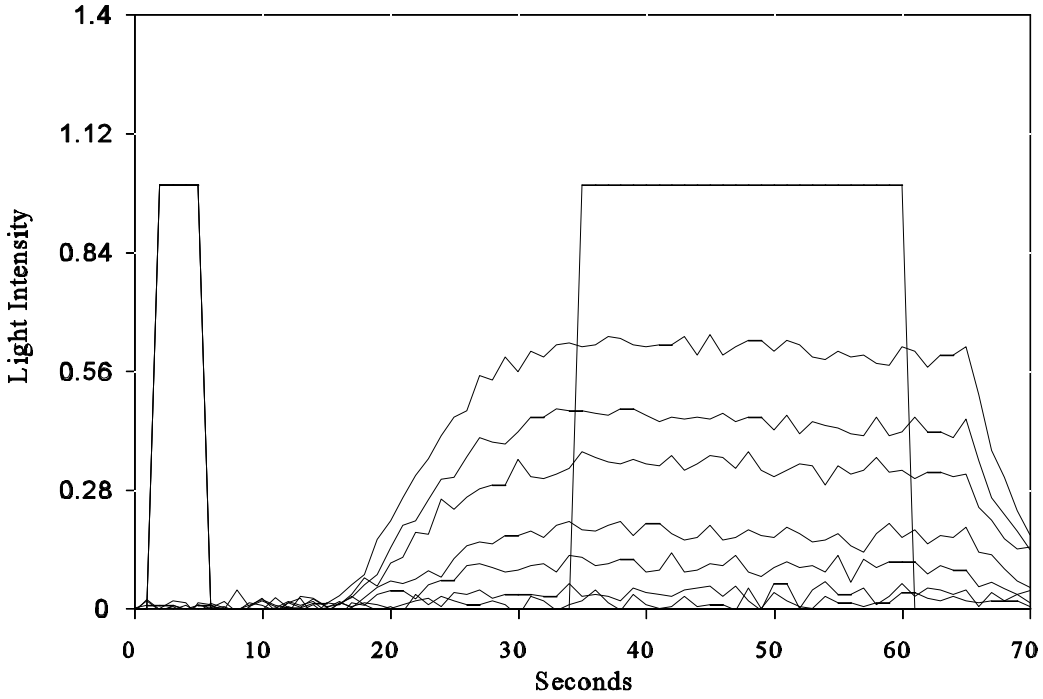

Figure 3.37. Small ByT-FAS system raw data output of light production from luciferase activity with increasing ATP concentrations.

Raw data traces of luciferase light production at different ATP concentrations. Increasing signal corresponds to increasing ATP concentration at the point of detection. Reagent and sample carrier stream flow ratios of 10/1. 10 *u*Ls of ATP sample injected in sample carrier flow stream. Luciferase and luciferin injected into the reagent carrier stream. HPLC fluorometer used as detection system with light source turned off and face plate of flow cell removed. Flow cell dimensions were 0.45 mm i.d. by 2 cm long.

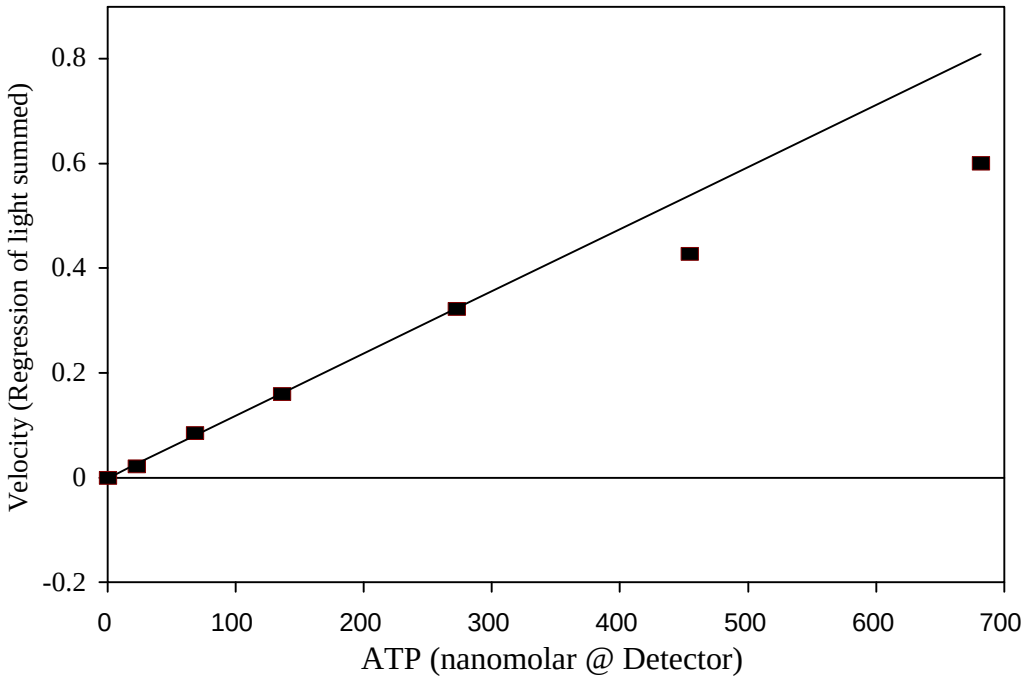

Figure 3.38. Small ByT-FAS system generated standard curve of ATP with luciferase.

Luciferase velocity is determined by performing a regression analysis on the summed light signal during the trapping phase of the run for each concentration of ATP. The linear range of the luciferase standard curve is 9.7 - 275 nM ATP at the point of detection. The R^2 for the linear range is 0.999. — Regression line.

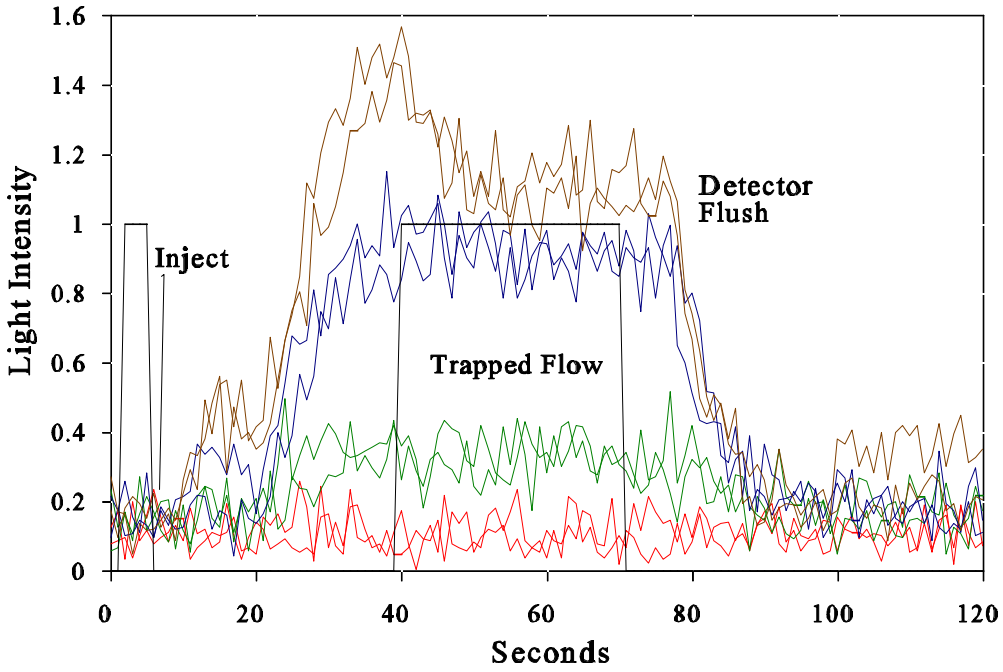

Figure 3.39. Small ByT-FAS system raw data traces for whole *E.coli* cell luciferase light production.

Four overnight cultures of *E. coli* containing the luciferase plasmid were grown overnight with different levels of tetracycline added to the growth media. The overnight cultures were diluted into fresh LB media to an approximate absorbance (600 nm) reading of 0.1. 150 *u*L of each culture was injected in the reagent side of ByT-FAS. 25 *u*L of 1 mM luciferin was injected in the sample side. Raw data traces of injected cultures contain the following amounts of tetracycline in the overnight growth media;
—— 0 ng/mL, —— 50 ng/mL, —— 75 ng/mL, —— 100 ng/mL tetracycline.

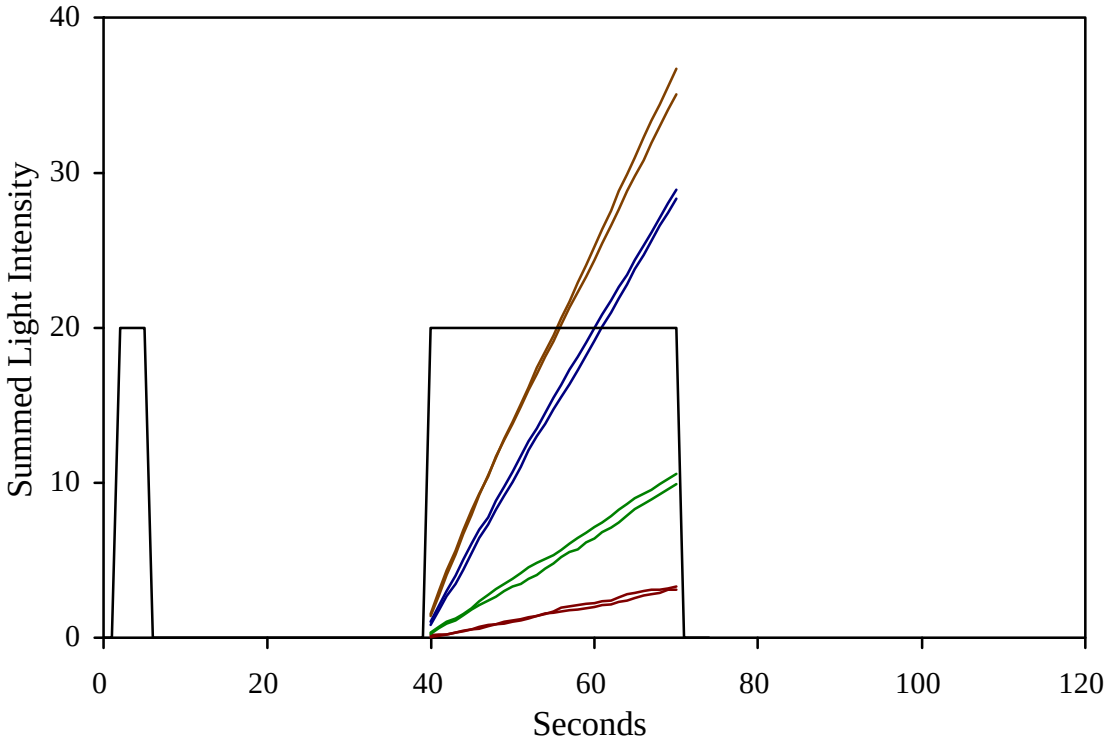

Figure 3.40. Summed Light Intensities for Whole *E. coli* cell Light Production.

From Figure 3.39 it is not easy to calculate a rate of light production for luciferase. Since light is a transient product of the enzyme luciferase, a summation of the light signal would provide a cumulative total of light produced. The approximately linear lines can then be used for regression analysis to determine a rate of light production. The pairs of lines correspond to the summed light signals of each overnight culture during the trapped flow period of the ByT-FAS run. The different colors represent the cultures with tetracycline in the overnight growth media as follows; —— 0 ng/mL, —— 50 ng/mL, —— 75 ng/mL,
—— 100 ng/mL tetracycline.

data traces in Figure 3.39 was lessened. These linear plots offered a visible representation of light accumulation in the detector cell even though light exists transiently. From the summed light intensities in Figure 3.40, a rate of light production for luciferase can be calculated.

To determine a rate of light production in each injected cell culture, a regression analysis of the summed light intensities of Figure 3.40 was performed between 45 and 70 seconds in the run. All of the summed light regression analyses had an R^2 value of 0.99 or higher These rates of light production from the slope of the regression analysis then needed to be normalized to the amount of bacteria in the injected culture that produced the light production rate. To do this, the rate of luciferase light production was divided by the absorbance (600 nm) of each diluted cell culture.

The standard curve of luciferase velocity per injected AU_{600nm} versus tetracycline concentration in the overnight growth media is shown in Figure 3.41. The standard response curve has an R^2 value of 0.99.

Physical steady state signals for the injected whole cell cultures were not verified in these experiments. However, the ByT-FAS system still had adequate sensitivity for the analysis of luciferase in the whole cells.

We believe the ByT-FAS technique and instrumentation adds a new dimension to the analysis of bacterial cells with flowing streams. Furthermore, there appear to be many potential applications of such an assay system for the rapid analyses of promoter DNA sequences, altered promoters, transcription repressors, and environmental toxins.

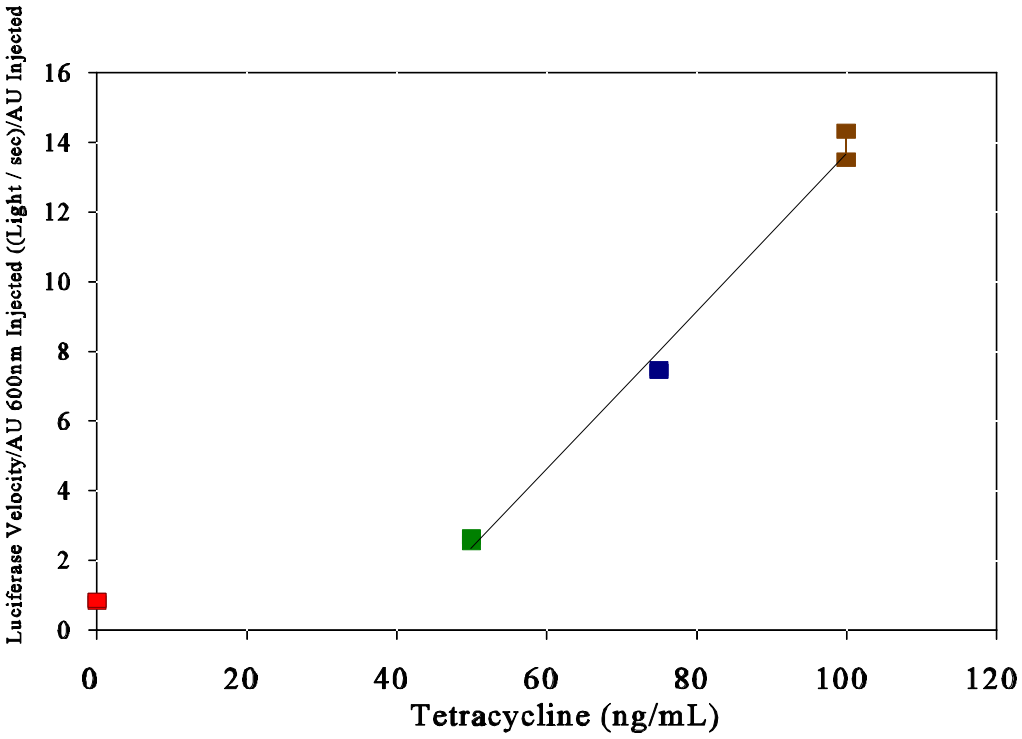

Figure 3.41. Standard curve of light production per injected AU_{600} versus tetracycline concentration.

From Figure 3.40 a regression analysis of each summed light intensity is taken between 45 and 70 seconds. This establishes a rate of light production (photons/sec) by luciferase. The rate of light production is then normalized for each cell culture by dividing the absorbance at 600 nm into the luciferase velocity. Once the luciferase velocities have been described by the number of bacteria assayed (based upon AU_{600nm}), the data are plotted versus the tetracycline concentration in the overnight growth media. The different colors represent the cultures with tetracycline in the overnight growth media as follows; ■ - 0 ng/mL, ■ - 50 ng/mL, ■ - 75 ng/mL, ■ - 100 ng/mL tetracycline. — Regression line.

Discussion

The technology driven society of today, with its ever increasing need for automation, has left at least one vocation behind. Biochemical research is still predominantly performed with test tubes, beakers, pipettors, and intensive manual manipulation. This is partly because some experiments are complex, with many individual steps. However, it is also a result of the shortcomings of existing laboratory automation equipment to address a majority of the concerns of the biochemical researcher all at one time. The needs of the biochemical researcher include but are not limited to; ease of use, low limits of detection, sensitivity, absolute measurements, small volumes, high sample throughput, low capital investment, and automated data handling.

ByT-FAS was designed to address the needs of the biochemical researcher for assay automation and to fill the existing void of current automated instrumentation.

Biochemical Measurements

Direct Measurements

Equivalent to better reproducibility than traditional manual measurements is the first test for any assay instrument for acceptance of its functionality. The spectrophotometric hemoglobin measurements with ByT-FAS shown in experiment 3.1 were intended compare ByT-FAS with manual cuvette measurements. As is shown in Table 3.1 and Figure 3.1 (Results), the ByT-FAS data have equivalent to better measurement precision with the same samples. This initial ByT-FAS precision test, makes its application to in-flow reaction chemistries a credible pursuit.

Non-enzyme Based Assays

Important to the biochemical community are the non-enzyme reaction chemistries for the determination of total protein in a sample. These include the biuret, bicinchinonic acid, and brom-cresol green assays to name a few. Because of the fast binding and color development for the brom-cresol green assay, it was chosen to test ByT-FAS for the determination of total protein compared with manual measurements in a series of the same standard solutions. As shown in Table 3.2 and Figure 3.2 (Results), the ByT-FAS data showed equivalent to better measurement precision and sensitivity compared with the manual cuvette assay, using the same samples.

By successfully testing ByT-FAS with direct measurement and non-enzymatic assays first, the extension of its application to enzyme assays in biochemistry, and its comparison to existing assay systems (FIA, segmented flow, centrifugal fast analyzers) is a logical next step.

Instrumentation and Enzymes

Measurements using enzymes is a frequent occurrence in biochemical research. However, the use of enzymes to quantitate metabolite concentrations or the kinetic characterization of the enzymes themselves is still usually performed manually. While the centrifugal fast analyzer can be used for absolute measurements, the significant capital investment as well as the lack of complete automation has limited its usefulness to clinical chemistry applications.[48] For flow injection analysis systems, acceptance in biochemical research has been limited by the restricted linear ranges and the inability to reach physical steady state as a result of the diluting affects of laminar flow. We believe that the inability of FIA to make absolute measurements is the primary reason for its lack of acceptance by the biochemical

community.

The main application of flow injection analysis in conjunction with enzymes has been the detection of enzyme activities.[49-51] In recent years, the use of immobilized enzyme reactors have also been successfully developed to quantitate metabolite concentrations with FIA.[52]

ByT-FAS and Enzymes

Alkaline Phosphatase Kinetic Characterization

To test ByT-FAS for enzyme kinetic characterization, a one-enzyme, one-substrate spectrophotometric reaction was chosen as a model enzyme assay. In addition to measuring the enzyme velocities with the ByT-FAS flow system, the assay was also performed manually with the same samples for direct comparison of the kinetic data.

Initial ByT-FAS kinetic data for alkaline phosphatase did not compare well with the manually generated as shown in Figures 3.4 - 3.7 (Results). This did not support the theory that ByT-FAS performed assays equivalent to those done manually. However, after correcting for exact flow rate contributions (in-flow dilution) and a non-specific protein binding phenomenon with the system tubing, the ByT-FAS data and the manual cuvette assay data were virtually identical as shown in Figures 3.8 and 3.9 and Table 3.3.

The in-flow characterization of enzyme kinetic parameters using ByT-FAS with small sample and reagent volumes is a first for FIA type systems.

Coupled Enzyme Fluorescent Assay for Hexokinase Kinetic Parameters

To test ByT-FAS with more complicated enzyme kinetic assays and different detection methods, a coupled enzyme assay with fluorescence detection was attempted. The model coupled enzyme reaction chosen was hexokinase coupled to glucose-6-phosphate dehydrogenase with fluorescence detection. The kinetic parameters, Kms for glucose and ATP with hexokinase and the Ki of ADP for ATP were determined using ByT-FAS and compared to known literature values. As shown in Table 3.4 (Results) the ByT-FAS generated kinetic data compare well with previously reported data in the literature.

ByT-FAS, because of its small volume physical steady state measurements, should have broad application to measurements using enzymes. Realistically, almost any conventional assay system that can be performed manually in test tubes and cuvettes could be designed for use with ByT-FAS. As a result, the biochemical researcher should finally be able to perform enzyme measurements without compromising any aspect of the original assay system. Most importantly, the knowledge of analyte concentration at the detection cell from the physical steady state measurements using small sample volumes (10 -25 *u*L), makes ByT-FAS ideally suited to the characterization of enzyme kinetic parameters.

Calibration of the Age of an Enzyme Reaction in ByT-FAS

The Michaelis-Menten equation is based on the assumption of measuring initial enzyme velocities and absolute knowledge of the reactant concentrations. For a manually performed reaction, the amount of time that elapses from the addition of enzyme to the substrate, mixing, and insertion of the reaction into the detector is at least a few seconds (2-5 seconds).

In ByT-FAS, the time required to attain physical steady state conditions of injected substrate and enzyme is **not** related to the age of an enzyme reaction at the point of trapping. It became apparent that the age of an enzyme reaction performed with ByT-FAS was an important variable to determine.

As a result, a one enzyme, two substrate reaction was chosen as a model to determine the age of an enzyme reaction in ByT-FAS. The enzyme was yeast glucose-6-phosphate dehydrogenase and the two substrates were β-glucose-6-phosphate and $NADP^+$.

From this type of experiment, the amount of product produced at physical steady state (trapping valve fired) is proportional to the age of enzyme reaction. The enzyme kinetic velocity during the trapped phase of the ByT-FAS run establishes the rate of product production. From this, the fluorescence signal difference between the enzyme blank and the reaction at physical steady state signal divided by the reaction rate gives the age of the reaction in seconds. From Figure 3.29 (Results), the age of an enzyme reaction in ByT-FAS was determined to be approximately 3 seconds.

ByT-FAS and Enzyme Kinetic Based Metabolite Quantitation

In addition to the characterization of enzyme kinetic parameters, ByT-FAS was tested with another enzyme application. The quantitation of glucose using yeast hexokinase coupled to glucose-6-phosphate dehydrogenase with a kinetic based standard curve has been successfully demonstrated with ByT-FAS (Figure 3.31, Results). The approximate first-order region of the Michaelis-Menten plot for glucose with hexokinase served as the linear range for the assay.

The ByT-FAS enzyme kinetic working assay was then tested with two different sample matrices for interference of the matrix on the assay chemistry. The mixed-diet food matrix showed interference while the canine heparinized plasma matrix did not (Figures 3.33 and 3.34 respectively, Results). The mixed-diet food matrix contains a mixture of sugars that could possibly interfere with the glucose binding to hexokinase. The food matrix interference is probably a result of competitive binding of the food matrix sugars for the glucose binding site on hexokinase. Alternatively, the canine heparinized plasma matrix contains only glucose as the predominant monosaccharide, which is why it displayed no interference with the enzyme assay. As shown in Table 3.9, the heparinized canine plasma glucose data generated with ByT-FAS was comparable to the data from the veterinary school method.

Other kinetic based metabolite measurements with existing manual methodologies could be adapted to ByT-FAS. However, before any assay system can applied to complex matrices, it must be tested for matrix interferences. This is especially the case for enzyme kinetic based quantitation because the measured initial rate is subject to significant interference if there are structurally similar compounds that could inhibit the enzyme in the matrix.

ByT-FAS and Enzyme Equilibrium Based Metabolite Quantitation

A plethora of enzyme equilibrium end-point assays for analyte quantitation exist in the literature and are commercially available from vendors like Sigma (St. Louis, MO). However, these diagnostic assay systems are almost always accompanied by a long incubation period (15-45 minutes) for the enzymes to catalyze the reaction to equilibrium.

From enzymological theory it is known that increasing the amount of enzyme concentration directly affects the speed of achieving equilibrium as long as the catalytic properties of the enzyme are not effected at the higher concentrations. Therefore, if the concentration of enzyme is increased, the incubation period required to achieve equilibrium could be reduced dramatically, possibly to as short as several seconds (less than a minute).

Because ByT-FAS uses significantly smaller volumes of substrate and enzyme than an equivalent manual assay system, the increased cost of consuming more enzyme (higher concentrations) is lessened.

This would enable the achievement of reaction equilibrium to be much faster using ByT-FAS without increasing the cost of analysis.

The assay system chosen to investigate the fast enzyme equilibrium assay with ByT-FAS was a cholesterol measurement catalyzed by cholesterol oxidase coupled to horseradish peroxidase with production of a fluorophore. Cholesterol samples were dissolved in 95 percent ethanol and the reagent was dissolved in buffer (experiment 2.15). The ByT-FAS generated data showed attainment of fast reaction equilibrium. However, ByT-FAS displayed indications of significant sample contaminations between runs. This phenomenon was never observed under routine operation for any other assay performed on the system. It may be attributable to the precipitation of the cholesterol in the flow system when it was mixed with the aqueous buffer that contained the enzyme reagent mixture. When the cholesterol and enzyme reagent mixture were combined in a test tube in the same ratios as in ByT-FAS, a precipitate formed.

Nevertheless, the potential for fast equilibrium enzyme measurements with ByT-FAS was shown to hold promise. The cholesterol assay system was not studied further.

Chemiluminescence and ByT-FAS

ByT-FAS Assay for ATP with Firefly Luciferase

The trend in biochemical research is an increasing need for sensitive analyses. As a result, ByT-FAS was examined for its application to chemiluminescent measurements. The assay system chosen was the hydrolysis of ATP to ADP by firefly luciferase with the concomitant production of light. A standard HPLC fluorometer without the light source turned on and direct exposure of the flow cell to the photomultiplier tube was used as a chemiluminometer. The working linear range of this assay system was established to be 9.75-275 nM ATP at the point of detection as shown in Figure 3.38. With a ByT-FAS reagent to sample carrier flow stream ratio of 10/1, this linear range corresponds to 0.11 - 3.03 *u*M of injected ATP concentration. The linear range of this assay could be made to incorporate lower concentrations of ATP with a better chemiluminescence detector. Nevertheless, the functional linear range of the working ByT-FAS assay is satisfactory for an application to sensitive ATP analyses.

ByT-FAS Chemiluminescent *E. Coli* Genetic Transcription Assay

Biochemists, molecular biologists, and biotechnologists frequently study changes in promoter sequences, transcription inducers and repressors, and growth media additives for their impact on the level of transcription of a certain gene. The laboratory standard quantitative procedure for elucidating the level of gene transcription in a cell is the method by Miller.[53] The general procedure for this assay relies on the amount of β-galactosidase that has been produced to serve as the reporter enzyme for a certain transcriptional event. The simplistic version of the procedure is described:

1. Prepare overnight cultures with different assay variable grown at 37^{O}C.
2. Dilute cells 1/100 into same media that they were grown in.
3. Grow diluted cells about 2 hours at room temperature until A_{600} is 0.7.
4. Set cells on ice
5. Spin down 1.5 mL of each culture and resuspend in 1 mL of assay buffer and place back on ice.
6. Dilute cells 1/6 into assay buffer and take absorbance of cells at A_{578}.

Assay for β-galactosidase

7. Place X *u*L of cells in assay buffer, plus 20 *u*L of 0.10% SDS, plus 10 *u*L of 2N NaOH, plus assay buffer to 800 *u*L total volume.
8. Incubate at 28-30^{O}C for 10 minutes for cell lysis.
9. Add 160 *u*L of 4 mg/mL ONPG (*o*-nitrophenyl galactoside) at time = 0.
10. Add 400 *u*L of 1M Na_2CO_3 after about 10-15 minutes and yellow color has developed. This stops the reaction.
11. Spin down assay mixture to remove cell debris for 2 minutes.
12. Measure absorbance at 420 nm.

Using this method, approximately 30 to 50 overnight cultures can be assayed in one full day.

Recently, a plasmid containing the firefly luciferase gene has been constructed and inserted into *E.coli*.[54] This recombinant *E.coli* strain was obtained as a gift from Dr. Timothy J. Larson for investigation of the ability to inject whole intact bacterial cells into ByT-FAS and quantitate the level of luciferase gene transcription under a tetracycline inducible promoter. Using tetracycline concentrations of 0, 50, 75, and 100 ng/mL in the overnight LB growth media, the diluted cell cultures were then injected into ByT-FAS using the same chemiluminescence detection system described above for the assay of ATP. The amount of light produced from the injected culture would indicate the amount of luciferase present in the injected culture and correspond to the level of genetic transcription at each tetracycline level. The data were normalized to the concentration of bacterial cells injected as determined by the absorbance of the injected culture at 600 nm. The method to determine the level of luciferase gene transcription using ByT-FAS is as follows.

1. Grow overnight cultures with different assay variable at 37^{O}C.
2. Cool cultures at room temperature for 2 hours.
3. Dilute culture 1/25 into fresh LB media.
4. Take absorbance of diluted culture at 600 nm versus LB blank.
5. Inject 150 *u*L of diluted culture into the reagent side of ByT-FAS and 25 *u*L of 1 mM luciferin substrate into the sample side of ByT-FAS.
6. Store light production data in spreadsheet and analyze.

Using this recombinant *E.coli* strain with luciferase as the reporting enzyme for gene transcription, and ByT-FAS as the assay instrument with chemiluminescent detection, the potential sample throughput each day can be well over 100. It is believed that this simpler assay system for studying genetic transcription will have broad appeal over the method of Miller. However, a more rigorous investigation of the ByT-FAS chemiluminescent assay method needs to be conducted before this assay can be recommended for routine use.

Existing Cell Based Flow Injection Analysis

Flow cytometry is a well established field with a large literature base. However, flow injection analysis has been applied to the analysis of injected cells in recent years and the new field has been called flow injection cytometry (cytoanalysis).[55-57] A large area of application in this field of instrumentation has been directed towards the coupling of a flow injection system to cell culture batches for on-line monitoring of microbial activity, intracellular enzyme activities, and metabolite concentrations in the culture. [48,58,59] For the on-line monitoring of intracellular enzyme activities, the flow injection system

employed an on-line cell disintegration mechanism through the action of ultrasonic and glass microbial-mixer mills.[49,50] In addition to the cell disintegration device, the flow injection manifold also contained a membrane device to separate the cell debris and the released enzyme from the disintegrated sample solution. In this manner the enzyme activities could be determined.

Flow injection cytometry manifolds have also been developed and demonstrated to perform on-line staining of DNA in trout erythrocytes with 4', 6-diamidino-2- phenylindole.[60] The erythrocyte cells were treated with 1.4% Nonidet NP-40 to facilitate penetration of the cell membranes. Also, the same flow injection manifold which used a mixing chamber and a highly viscous sucrose carrier solution to lessen laminar flow of the sample and reagent out of the mixing chamber, was used to determine the Km of glutathione-S-transferase with the chromogen monochlorobimane. However, the determined Km was not similar to previously published values reportedly because of cell heterogeneity.

It seems that ByT-FAS is the only method reported to date for in line evaluation of enzymes at physical steady state.

Instrumentation

Instrument Variables Affecting Physical Steady State

Laminar flow is a phenomenon that exists in every pressure driven non-turbulent pumping system (except electroosmotic flow). Even though it cannot be eliminated entirely for non-turbulent flow, the physical parameters that contribute to its magnitude can be manipulated to lessen its effects.

Several publications have attempted to describe the degree to which the flow system parameters, L (tubing length), q (flow rate), a (inner radius), and D (diffusion coefficient of the injected analyte) contribute to laminar flow.[7,61] Vanderslice *et al* dealt mainly with theoretical mathematical derivations for describing the flow system parameter effects on bolus dilution during flow transport, while Gomez-Nieto *et al* empirically deduced the flow parameter effects. Nevertheless, while the degree of contribution of each flow parameter can be debated, the contribution of each parameter relative to one another is in agreement. The most significant contributor to laminar flow is the tubing inner radius, and secondly, the tubing length from the injector to the detector (including the injection loop and the detector cell dimensions). Flow rate and molecular diffusion coefficient also play a rule in laminar dispersion, but to a lesser extent. Therefore, if a flow system is to circumvent the effects of laminar flow and achieve a physical steady state detector signal, the tubing inner radius and length must be reduced between injection and detection as much as possible. Also, wherever possible the system tubing should be braided or knotted to destroy the laminar flow profile. The main underlying design feature of ByT-FAS that has not been applied in flow injection analysis to this point is the reduction of system tubing inner radius and length**.** As a result, ByT-FAS is the first solely dedicated flow instrument embodiment designed to make physical steady state measurements.

Physical Steady State

The concept of a physical steady state bolus profile is fundamental to the flow injection, and chemical analyzer community.[4] Excluding fast kinetic stopped flow analyzers, which are not amenable to automation and require large sample and reagent volumes (1-3mL),[15] physical steady state measurements have not been reported for routine measurements with conventional flow injection systems.

Physical steady state detector signals have been mathematically computed for flow injection analysis. Recent publications have presented mathematical models to compute what the physical steady

state signal would be if a large enough sample and reagent volume were injected to saturate the system.[30,34] In a flow injection system, physical steady state measurements would result in lower limits of detection, longer linear ranges, and increased sensitivities. The miniature design of ByT-FAS, specifically in tubing internal diameter and tubing length, appears to be the first enabling instrument for physical steady state measurements, which have unequivocal advantages over traditional flow injection analysis signal profiles. The most relevant benefit to the biochemical researcher is the simple calculation of the concentration of sample and reagent at the point of detection from the knowledge of the injected concentration.

Concentration at the Point of Detection

At physical steady state, where the concentration of the sample/reagent mixture is not affected by laminar dispersion, the concentration of the sample at the detection cell (prior to any chemical reaction) is as shown in equation 4.1 and the concentration of the reagent at the detection cell (prior to any chemical reaction) is as shown in equation 4.2 .

$$[SD_c] = [S^0] * \text{CS Flow}\backslash(\text{TS Flow}) \qquad (4.1)$$

$$[RD_c] = [R^0] * \text{RS Flow}\backslash(\text{TS Flow}) \qquad (4.2)$$

Where SD_c is the steady state concentration of the sample at the detector and RD_c is the steady state concentration of the reagent at the detector; S^0 is the original concentration of the sample placed in the sample loop of the SIV; CS Flow is the flow rate of the carrier stream, R^0 is the original concentration of the reagent placed in the reagent loop of the SIV, RS Flow is the flow rate of the reagent stream, and TS Flow is the total system flow rate.

The ability to compute the measured concentrations of the sample and reagent from the direct knowledge of the injected concentrations is an important feature and makes possible the determination of absolute attributes of chemical/biochemical compounds and chemical/biochemical reactions.

Determination of Physical Steady State

The general definition of physical steady state is the saturation of a flow system with a large enough volume that an analyte appears in the detector undiluted by the effects of flow transport. This seems to be a simple definition. However, determining when an injected analyte reaches physical steady state in the detector cell has not been rigorously defined in the literature: probably because no one has made physical steady state measurements routinely until now. We used three different approaches to unambiguously determine a physical steady state signal.

First, an analyte can be measured manually external to the flow system; then, based upon the sample and reagent carrier flow stream ratios and the use of equations 4.1 and 4.2, the concentration (signal) of the analyte at physical steady state can be predetermined before injection. When the detector signal from the injected analyte reaches the precalculated value, the analyte can be said to be at physical steady state. For example, if an analyte has a manual absorbance reading of 0.5 and a flow system has a sample carrier stream flow rate of 0.5 mL/min with a total flow rate of 1 mL/min, then from equation 4.1 the physical steady state signal of the injected analyte should be 0.25 absorbance units. From this type of an experiment, the time it takes for an injected analyte to reach physical steady state and the duration of the absolute signal can be easily determined. If the analyte never reaches the predetermined detector

signal, it can be concluded that it never achieved physical steady state.

Second, an analyte can be used as the carrier stream in the flow system to saturate the system tubing. The detector output while the system is saturated with the analyte can be used as the physical steady state benchmark signal. The system can be flushed of the analyte to achieve a baseline detector signal and then injections of the same analyte concentration can be made to determine when the analyte reaches physical steady state and its duration. This is the technique that was used to determine the attainment of physical steady state in experiment 2.5 (Figures 3.21 and 3.22, Results). While this technique establishes the physical steady state signal absolutely, it is time consuming to perform and requires a large volume of analyte.

Any change of a system component or operational parameter such as tubing diameter, detector cell, sample loop, flow rates or different molecular weight analyte will affect the attainment of physical steady state. Consequently, this is not a good routine validation technique to use for calibration of an absolute measurement in a flow system.

Third, an empirical determination of physical steady state attainment can be used. Without exception, the maximum obtainable detector signal of an analyte at a saturation volume injected into any fixed configuration flow system is the signal at a physical steady state concentration. Increasing the injected volume for a fixed configuration flow system beyond that necessary to attain physical steady state will only result in a longer duration of the absolute measurement signal, not an increase in the signal itself. Therefore, the detector signal as a function of injected sample volume can be used to determine the minimum injectable volume necessary to achieve physical steady state in the detector cell. The assay of detector signal as a function of injected volume is a straightforward approach to determine the volume necessary to reach an absolute measurement.

The following procedure was used to elucidate when a given volume of injected analyte reaches physical steady state, if at all, and for how long.

Using a triplicate injection of a tracer volume that reaches a reproducible maximum signal for a minimum of 20 seconds, determine the time interval that physical steady state is achieved by signal values that are 99+ percent the maximum detector output. Using this time interval, calculate the average physical steady state signal for all raw data traces and define that average signal as the value for 100% physical steady state. Convert the raw data traces to percent of physical steady state by dividing each signal data point by the average signal at physical steady state. Smooth out the percent of physical steady state data by making a moving box-car average of the data in the form of (00X00). Determine the standard deviation of the data over the same time interval as the average physical steady state signal described above. Average the standard deviations calculated from each set of smoothed data. Determine the percentage value of -1σ, -2σ, -3σ, and $+1\sigma$, $+2\sigma$, $+3\sigma$ standard deviations away from 100% physical steady state. When a different tracer volume is injected, and the detector signal enters the zone above -2σ standard deviations away from 100% physical steady state, it cannot be statistically excluded from having reached physical steady state. As long as the signal varies between $+3\sigma$ and -3σ standard deviations of the 100% signal, without a noticeable trend, the sample bolus can be considered at physical steady state.

Depending on the variance of the detector output data at the defined physical steady state signal, the value of 1σ away from physical steady state expressed as percentage will be variable. However, for the small ByT-FAS system, the approximate value of 1σ away from physical steady state expressed as a percentage was 0.9% as shown in Figure 3.22.

This technique was employed to study the effects of reagent to sample carrier stream flow ratio and sample side tubing internal diameter variations in experiments 2.6 - 2.11.

ByT-FAS and Physical Steady State

Using the empirical physical steady state determination in experiments 2.6 -2.11, different sample side tubing diameter reductions, different reagent to sample carrier stream flow ratios, and different molecular weights of injected analytes, all affected the time of attainment and duration of physical steady state in ByT-FAS.

The observed affects on physical steady state of the different system variables in experiments 2.6-2.11 were consistent with the equations of Vanderslice *et al* as described in detail above (equation 1.1, Introduction).

Sources of Detector Signal Variation

The signal at physical steady state has inherent variance associated with it. It has been observed in this work, as well as others, that the positive displacement syringe pump can produce pulsed flow as a result of the mechanical stepping motor.[60] It had also been observed that the syringe plungers used in the small ByT-FAS design did not always move continuously down the syringe barrel. They had been observed to stick at some points and produce lapses and then surges in flow rate. This would cause signal variance at the point of detection. To reduce this effect, silicone grease was applied to the syringe plunger tip to lessen the friction of the plunger gasket on the syringe barrel. This produced a visibly more continuous, even flow rate.

Future Research for ByT-FAS

The potential of ByT-FAS to automate routine biochemical assays in the laboratory is significant. As more applications to different assay systems accumulate, its prevalence as a tool for the biochemist should increase.

Furthermore, research directed toward improvements of the fundamental concept of the ByT-FAS design show promise. Specifically, a ByT-FAS flow system that is micro-machined onto the surface of a silicon chip like capillary zone electrophoresis systems will enhance the basic concept of the design. Using micro-engraving techniques, the internal diameters of the flow channels (injection loops, transport channels, and detector flow cells) and the total flow system volume can be reduced even further than is currently feasible. In addition to the flow channels, other instrument components such as a magnetically driven rotary pump, system electronic control, and flow cells are currently being developed on the chip for FIA systems.[62] Advances such as these will produce systems that require even less sample and reagent volume to reach physical steady state than is presently needed. These even smaller systems will produce greater laboratory economy of sample and reagent (consumption and waste) without compromising the measurement process.

References

1. Stillwell, J.A. *J. Clin. Pathol.* **1981**, *34*, 589-594.

2. Broughton, P.M.G.; Hogan, T.C. *Ann. Clin. Biochem.* **1981**, *18*, 330-342.

3. Craig, T.M. *J. Auto. Chem*. **1980**, *2*, 31-33.

4. Růžička, J.; Hansen, E.H. *Flow Injection Analysis*; John Wiley & Sons: New York, 1981; pp 1-4.

5. Stewart, K.K.; Beecher, G.R.; Hare, P.E. *Fed. Proc. Fed. Am. Soc. Biochem*. **1974**, *33*, 1429.

6. Růžička, J.; Hansen, E.H. *Anal. Chim. Acta* **1975**, *78*, 145-147.

7. Vanderslice, J.T.; Stewart, K.K.; Rosenfeld, A.G.; Higgs, D.J. *Talanta* **1981**, *28*, 11-18.

8. Skeggs, L.T. *Am. J. Clin. Pathol*. **1957**, *13*, 451.

9. Anderson, N.G. *Science* **1969**, *166*, 317-324.

10. Valcarcel, M.; Luque de Castro, M.D. *Flow Injection Analysis, principles and applications*; Ellis Horwood: England, 1987; pp 7-38.

11. Stewart, K.K.; Hillard, S.W. *Talanta* **1997**, Submitted for publication.

12. Smith, P.K.; Krohn, R.I.; Hermanson, G.T.; Mallia, A.K.; Gartner, F.H.; Provenzano, M.D.; Fujimoto, E.K.; Goeke, N.M.; Olson, B.J.; and Klenk, D.C. *Anal. Bioch.* **1985**, *150*, 76-85.

13. Anderson, N.G. *Anal. Bioch*. **1968**, *23*, 207-218.

14. *Anal. Chem*. **1985**, *57*, 651-668 A.

15. Gibson,Q. H.; In *Methods in Enzymology Vol. XVI*; Kustin, K., Ed.; Series Ed.; Colowick S. P.; Kaplan, N. O.; 1969, p 187-228.

16. Karlberg, B.; Pacey, G.E. *Flow Injection Analysis, A practical guide*; Elsevier Science Publishers: New York, 1989; pp 1-65.

17. Růžička, J. In *Flow Injection Analysis (FIA) Based on Enzymes or Antibodies;* Schmid, R.D., Ed.; VCH Publishers: New York, 1991; p 3.

18. Moller, J. *Flow Injecion Analysis*, Springer Verlag: Heidelberg, 1988.

19. *Flow Injection Atomic Spectroscopy;* Burguera, J.L., Ed.; Marcel Dekker: New York, 1989.

20. *Flow Injection Anlalysis (FIA) Based on Enzymes or Antibodies*; Schmid, R.D., Ed.; VCH Publishers: New York, 1991.

21. Vanderslice, J.T.; Rosenfeld, A.G.; Beecher, G.R. *Anal. Chim. Acta* **1986**, *179*, 119-129.

22. Růžička, J.; Hansen, E.H. *Flow Injection Analysis*; John Wiley & Sons: New York, 1981; pp 31-50.

23. Levenspiel, O. *Chemical Reaction Engineering*, 2nd Ed., Wiley: New York, 1972.

24. Taylor, G. *Proc. R. Soc. London, Ser. A.* **1953**, *219*, 186.

25. Tijssen, R. *Anal. Chim. Acta* **1980**, *114*, 71-89.

26. Ananthakrishnan, V.; Gill, W.N.; Barduhn, A.J. *AIChEJ*. **1965**, *11*, 1063.

27. Ramsing, A.; Růžička, J;.Hanson, E. H.; *Anal. Chim. Acta* **1980**, *114*, 165-181.

28. Valcarcel, M.; Luque de Castro, M.D. *Flow Injection Analysis, principles and applications*; Ellis Horwood: England, 1987; pp 275-284.

29. Blanco,M.; Coello, J.; Iturriaga, H.; Maspoch, S.; Riba, J. *J.F.I.A.* **1990**, *7*, 3-10.

30. Zhang, C.; Narusawa, Y.; Kitahama, S.; *Chem. Lett.* **1993**, 877-880.

31. Betteridge, D. *Anal. Chem*. **1978**, *50*, 832A-846A.

32. Chalk, S.J.; Tyson, J.F. *Anal. Chem*. **1994**, *66*, 660-666.

33. Jordan, J.M.; Love, M.D.; Pardue H.L. *Anal. Chim. Acta* **1993**, *272*, 125.

34. Roussin, J.A.; Li, J.; Pardue, H.L. *Anal. Chim. Acta* **1995**, *303*, 199-210.

35. Korenaga, T.; Shen, F.; Yoshida, H.; Takahashi, T.; Stewart, K.K. *Anal. Chim. Acta* **1988**, *214*, 97-105.

36. van der Linden, W.E. *Anal. Chem*. **1987**, *6*, 37-40.

37. *Methods of Enzymatic Analysis*, 3rd ed.; Bergmeyer, H.U., Ed.; Verlag Chemie: Deerfield Beach, 1983; Vol. 1, pp 15-21.

38. *Methods of Enzymatic Analysis*, 3rd ed.; Bergmeyer, H.U., Ed.; Verlag Chemie: Deerfield Beach, 1983; Vol. 1, p 166.

39. Pardue, H.L. *Clin. Chem*. **1977**, *23*, 2189-2201.

40. Wilkinson, J.T. *Clin. Chem*. **1965**, *11*, 239.

41. Mottola, H.A.; Perez-Bendito, D.; *Anal Chem.* **1994**, *66*, 131-162 R.

42. Giang, P.G. In *Methods in Enzymatic Analysis*, Bergmeyer, H.U., Ed.; Verlag Chemie: New York, 1974; pp 2249-2259.

43. Stenesh, J. *Core Topics in Biochemistry*; Cogno Press: Michigan, 1993; pp 221-264.

44. *Methods of Enzymatic Analysis*, 3rd ed.; Bergmeyer, H.U., Ed.; Verlag Chemie: Deerfield Beach, 1983; Vol. 1, pp 163-170.

45. Chang, R. *Physical Chemistry with Applications to Biological Systems*, Macmillan: New York, 1981; pp 348-389.

46. Fromm H.J.; Zewe V.; *JBC* **1962**, *237*, 3027-3032.

47. Barman, T.E.; *Enzyme Handbook*, Springer: New York, 1969; p 377.

48. *Centrifugal Analysers in Clinical Chemistry*; Price, C.P.; Spencer, K., Eds.; Praeger: New York, 1980.

49. Steube, K.; Spohn, U. *Anal. Chim. Acta* **1994**, *287*, 235-246.

50. Steube, K.; Spohn, U. *J. Biotechnology* **1994**, *33*, 221-231.

51. Luque de Castro, M.D.; Fernández-Romero, J.M. In *Flow Injection Analysis (FIA) Based on Enzymes or Antibodies;* Schmid, R.D., Ed.; VCH Publishers: New York, 1991; p 135.

52. Matsumoto, K. In *Flow Injection Analysis (FIA) Based on Enzymes or Antibodies;* Schmid, R.D., Ed.; VCH Publishers: New York, 1991; p 193.

53. Miller, J.H.; *Experiments in Molecular Genetics*; Cold Spring Harbor Laboratory; Cold Spring Harbor, New York, 1972; pp 352-355.

54. Personal communication with Dr. Timothy J. Larson.

55. Růžička, J. *Analyst* **1994**, *119*, 1925-1934.

56. Lindberg, W.; Růžička, J.; Christian, G.D. *Cytometry* **1993**, *14*, 230-236.

57. Růžička, J.; Lindberg, W. *Anal. Chem.* **1992**, *64*, 537A-545A.

58. Ding, T.; Bilitewski, U.; Schmid, R.D.; Korz, D.J.; Sander, E.A. *J. Biotechnology* **1993**, *27*, 143-157

59. Huang, Y.L.; Li, S.Y.; Dremel, B.A.A.; Bilitewski, U.; Schmid, R.D. *J. Biotechnology* **1991**, *18*, 161-172.

60. Lindberg, W.; Scampavia, L.D.; Růžička, J.; Christian, G.D. *Cytometry* **1994**, *16*, 324-330.

61. Gomez-Nieto, M.A.; Luque de Castro, M.D.; Martin, A.; Valcarcel, M. *Talanta* **1985**, *32*, 319-324.

62. Pacey, G.E.; International Conference on Flow Injection Analysis, January 12-16, 1997, Orlando, Florida.

Appendix A.

Table A.1 **Existing assay instrumentation with comparison of operational parameters to ByT-FAS**

Comparison of existing instrumentation with ByT-FAS for the attributes of measuring absolute concentrations, approximate sample throughput, automation potential, and approximate sample volume required for analysis.

	Direct or Relative Measurements	Samples/ Hour	Automation	Approximate Sample Volumes
Segmented- Flow Systems	Direct	30-60	Yes	0.5-2mL
Robotics	Direct	60-200	Yes	1-2mL
Centrifugal Analyzers	Direct	20-100	No	200uL
Stopped Flow	Direct	10-30	No	1-5mL
FIA	Relative	30-300	Yes	10-100uL
Stopped Flow FIA	Relative	30-100	Yes	10-100uL
ByT-FAS	Direct	30-100	Yes	10-100uL

Vita

Stephen Wayne Hillard was born in Altoona, Pennsylvania, on May 4, 1969. He graduated from Hollidaysburg Area High School in June of 1987. That same year, he attended George Mason University, Fairfax, Virginia, and received his Bachelor of Science in Biology in May, 1992. That same year he entered the graduate program in the Department of Biochemistry at Virginia Polytechnic Institute and State University. He received his Doctor of Philosophy in Biochemistry in March 1997. Stephen Hillard married Katya W. Dass in June 1992. Upon graduation, they plan to settle in the Puget Sound area of Washington state.